

Modular transformations and topological orders in two dimensions

Fangzhou Liu,^{1,2} Zhenghan Wang,³ Yizhuang You,⁴ and Xiao-Gang Wen^{1,2,5}

¹*Perimeter Institute for Theoretical Physics, Waterloo, Ontario, N2L 2Y5 Canada*

²*Department of Physics, Massachusetts Institute of Technology, Cambridge, Massachusetts 02139, USA*

³*Microsoft Station Q, CNSI Bldg. Rm 2237, University of California, Santa Barbara, CA 93106, USA*

⁴*Institute for Advanced Study, Tsinghua University, Beijing 10084, China*

⁵*Institute for Advanced Study, Tsinghua University, Beijing, 100084, P. R. China*

The string-net approach by Levin and Wen and the local unitary transformation approach by Chen, Gu and Wen provides ways to systematically label 2+1D topological orders with gapped edge (which will be called exact topological order). In those approaches, different many-body wave functions for exact topological orders are described by different fixed-point tensors. Though extremely powerful, the resulting fixed-point tensors are many-to-one description of exact topological orders. As a result it is hard to judge if two different fixed-point tensors describe the same quantum phase or not. We want to improve that approach by giving a more physical description of the topological orders. We find that the non-Abelian Berry's phases, T - and S -matrices, of the topological protected degenerate ground states on a torus give rise to a more physical description of topological orders. It is conjectured that the T and S -matrices (up to an unitary transformation) form a complete and one-to-one characterization of exact topological orders and can replace the fixed-point tensor description to give us a more physical label for topological orders. As a result, all the topological properties can be obtained from the T - and S -matrices, such as number of quasiparticle types (from the dimension of the T or S), the quasiparticle statistics (from the diagonal elements of T), the quantum dimensions of quasiparticles, *etc*.

Contents

I. Introduction	1
II. Local unitary transformation approach and modular transformations	2
III. List of different topological orders	4
A. $N = 1$ loop states – the \mathbb{Z}_2 states	4
B. $N = 1$ string-net state – the “Fibonacci” state	8
C. An $N = 2$ string-net state – the “Pfaffian” state	10
D. Another $N = 2$ string-net state – the S_3 state	12
E. An $N = 2$ string-net state – the \mathbb{Z}_3 state	14
F. $N = 3$ string-net states – the \mathbb{Z}_4 states	15
G. More $N = 3$ string-net states – the $\mathbb{Z}_2 \times \mathbb{Z}_2$ states	18
H. An $N = 3$ string-net state – the “Chiral” state	19
IV. Summary	20
A. Ideal Hamiltonian for fixed-point states on a torus	21
References	23

I. INTRODUCTION

One of the most important questions in condensed matter physics is the description and the classification of different phases of matter. Landau's symmetry-breaking theory^{1,2} provides a very elegant answer to this question: different phases are characterized by different broken symmetries. Thus by classifying all different broken symmetries, we can get a classification of phases.

Though extremely powerful, Landau's theory fails to explain many new states found in experiments including the Fractional Quantum Hall(FQH) states.^{3,4} These new states thus bring up once again the old question of how to classify different phases of matter.

A closer look at Landau's symmetry-breaking theory reveals that the theory only describes direct-product states up to some small local perturbations (see Ref. 5). Since these small perturbations can only modify the direct-product states locally, Landau's theory can only describe states with “short-range entanglements”. Intuitively, these states can only account for a small fraction of all possible quantum many-body states. Thus what seems to be missing in Landau's theory is a large class of states with “long-range entanglement”. Those states were named topologically ordered states in 1989 before the concept of entanglements become popular.^{6,7} Different patterns of long-range-entanglements/topological-orders correspond to different quantum phases.

But what are these patterns of long-range entanglement? What are topological orders? It is hard to answer these questions since those patterns/orders are new concepts that do not even have a label. So to study topological-order/long-range-entanglement, we first need to invent labels or mathematical symbols for them. The first label/symbol invented is the ground state degeneracy $D_{\text{deg}}(g)$ on torus (with genus $g = 1$)¹⁰ and other Riemann surfaces.^{6,7} But it was clear from the beginning that this is not a very good label, since the same $D_{\text{deg}}(g)$ can correspond to many different topological orders. To obtain a better label, in Ref. 8,9, it was proposed to use the non-Abelian geometric phases¹¹ of degenerate ground states on Riemann surfaces to characterize different topo-

logical orders.

It was conjectured⁸ that the non-Abelian geometric phases (the non-Abelian part) form a complete and one-to-one description of topological orders. On torus, they are described by T - and S -matrices, which generate a projective representation of the modular transformation on the torus. We can view T - and S -matrices as some kind of “non-local order parameter”. Therefore, the concept of topological order is defined through the physical properties of robust ground state degeneracy (called topological degeneracy)^{6,7} and robust geometric phases induced by the modular transformation of the degenerate ground states,^{8,9} just like the concept superconducting order was introduced through physical properties of zero resistance and Meissner effect. This led to the establishment of the concept of topological order (and long-range entanglements). It is thus very desirable to develop a comprehensive theory of topological orders based on T - and S -matrices.

However, the current comprehensive theory of 2+1D *exact topological orders* (*ie* the topological orders that can have a gapped edge)² is not based on T - and S -matrices, but rather, based on the string-net approach of Ref. 12 and local unitary transformation approach of Ref. 5. They provide a systematic description of 2+1D exact topological orders by systematically labeling the corresponding “long-range entangled” many-body wave functions through a set of fixed-point tensors. These fixed-point tensors form a mathematical structure called tensor category theory. Since the many-body wave functions described by the fixed-point tensors are explicitly known, we can construct exactly soluble Hamiltonians to realize each topological order described by a fixed-point tensor.

Although the fixed-point tensors approach (*ie* the string-net or the local-unitary-transformation approach) is closely related to the many-body wave function, it is known that different fixed-point tensors can correspond to same quantum phase. To be more precise, the different fixed-point tensors actually describe different unitary fusion categories (UFC), and two different UFC’s will describe the same 2+1D topological order if they have the same Drinfeld center.[?]

So to better identify the quantum phases described by the fixed-point tensors, and in an attempt to develop a theory of topological orders based on T - and S -matrices, in this paper, we will calculate the T - and S -matrices from the fixed-point tensors. This allows us to identify various topological orders in the the many-body wave functions described by the fixed-point tensors. In particular, we can calculate the number of quasiparticle types, the quasiparticle statistics and quantum dimensions, *etc* .

II. LOCAL UNITARY TRANSFORMATION APPROACH AND MODULAR TRANSFORMATIONS

In this section, we will review the local-unitary transformation approach and associated fixed-point tensor description of many-body wave functions of topological ordered states. The key in the local unitary transformation approach is a new definition of equivalence class on many-body ground states. Two gapped many-body ground states were defined as belonging to the same equivalence class (*ie* the same “phase”) if and only if they are connected by a local unitary (LU) transformation defined as follows:

$$|\Phi(1)\rangle \sim |\Phi(0)\rangle \text{ iff } |\Phi(1)\rangle = \mathcal{T}[e^{-i \int_0^1 dg \tilde{H}(g)}]|\Phi(0)\rangle \quad (1)$$

where \mathcal{T} is the path-ordering operator and $\tilde{H}(g) = \sum_i O_i(g)$ is a sum of local Hermitian operators. It can be proved that the above definition is equivalent to the standard definition through “adiabatic evolution” (*ie* two states belong to the same phase if and only if they can be connected through a gapped adiabatic evolution).⁵ The new definition of equivalence class is advantageous because it provides a very operational way to determine if two states belong to the same phase, thus provides a very natural way for renormalization. Under this definition, “long-range entangled” states are those that are not in the same phase as direct-product states. Different “long-range entanglement” are then called “topological orders”.

Following the new definition of equivalence class, a wave function renormalization scheme can be introduced.^{5,12,13} It contains two basic moves called “F-move” and “P-move”, both of which are the generalized local unitary (gLU) transformations. Under this renormalization scheme, gapped ground states will only flow within the same equivalence class, *ie* renormalization does not change its topological order. Thus a fixed point in this renormalization scheme can be used to represent a whole equivalence class. Following the convention of Ref. 5, we represent the two renormalization moves at fixed point by tensors:

$$\Phi_{\text{fix}} \left(\begin{array}{c} i \quad j \quad k \\ \alpha \quad \beta \\ m \quad l \end{array} \right) \simeq \sum_{n=0}^N \sum_{\chi=1}^{N_{kjn^*}} \sum_{\delta=1}^{N_{nll^*}} F_{kln,\chi\delta}^{ijm,\alpha\beta} \Phi_{\text{fix}} \left(\begin{array}{c} i \quad j \quad \chi \quad k \\ \delta \quad n \\ l \end{array} \right),$$

$$\Phi_{\text{fix}} \left(\begin{array}{c} \beta \\ i \quad k \quad i \\ \alpha \end{array} \right) \simeq P_i^{kj,\alpha\beta} \Phi_{\text{fix}} \left(\begin{array}{c} i \end{array} \right), \quad (2)$$

also, the simplest fixed-point wave function was represented by:

$$\Phi_{\text{fix}} \left(\begin{array}{c} i \end{array} \right) = A^i = A^{i^*}. \quad (3)$$

The above-mentioned fixed point tensors can be obtained through solving a set of self-consistent equations. Since the fixed-point state will not change under renormalization, we can apply renormalization moves in arbitrary orders. This arbitrariness gives us a set of self-consistent conditions that fixed point tensors must satisfy. The self-consistent conditions are summarized below:⁵

$$N_{ikj} = N_{kji} = N_{i^*j^*k^*} \geq 0, \quad \sum_{j,k} N_{ii^*k} N_{jk^*j^*} \geq 1,$$

$$\sum_{m=0}^N N_{jim^*} N_{kml^*} = \sum_{n=0}^N N_{kjn^*} N_{l^*ni},$$

$$(F_{kln,\chi\delta}^{ijm,\alpha\beta})^* = F_{l^*i^*m^*,\beta\alpha}^{jkn,\chi\delta},$$

$$\sum_{n,\chi,\delta} F_{kln,\chi\delta}^{ijm',\alpha'\beta'} (F_{kln,\chi\delta}^{ijm,\alpha\beta})^* = \delta_{m\alpha\beta,m'\alpha'\beta'},$$

$$\begin{aligned} & \sum_t \sum_{\eta=1}^{N_{kjt^*}} \sum_{\varphi=1}^{N_{tin^*}} \sum_{\kappa=1}^{N_{lts^*}} F_{knt,\eta\varphi}^{ijm,\alpha\beta} F_{lps,\kappa\gamma}^{itn,\varphi\chi} F_{lsq,\delta\phi}^{jkt,\eta\kappa} \\ &= e^{i\theta_F} \sum_{\epsilon=1}^{N_{qmp^*}} F_{lpq,\delta\epsilon}^{mkn,\beta\chi} F_{qps,\phi\gamma}^{ijm,\alpha\epsilon}, \end{aligned}$$

$$e^{i\theta_{P1}} P_i^{kj,\alpha\beta} = \sum_{m,\lambda,\gamma,l,\nu,\mu} F_{i^*i^*m^*,\lambda\gamma}^{jj^*k,\beta\alpha} F_{m^*i^*\nu\mu}^{i^*mj,\lambda\gamma} P_i^{lm,\mu\nu},$$

$$e^{i\theta_{P2}} P_i^{jp,\alpha\eta} \delta_{im} \delta_{\beta\delta} = \sum_{\chi=1}^{N_{kjk^*}} F_{kllk,\chi\delta}^{ijm,\alpha\beta} P_k^{jp,\chi\eta}$$

for all k, i, l satisfying $N_{kil^*} > 0$,

$$\Phi_{\text{fix}} \left(\begin{array}{c} \bigcirc \\ i \end{array} \right) \equiv A^i = A^{i^*} \neq 0, \quad \sum_i A^i (A^i)^* = 1,$$

$$P_i^{mj,\gamma\lambda} A^i = e^{i\theta_{A1}} P_{j^*}^{m^*i^*,\lambda\gamma} A^j,$$

$$\Phi_{ikj,\alpha\beta}^\theta = e^{i\theta'} \sum_{m,\lambda,\gamma} F_{j^*im,\lambda\gamma}^{ijk^*,\alpha\beta} P_i^{mj,\gamma\lambda} A^i,$$

$$\Phi_{ikj,\alpha\beta}^\theta = e^{i\theta_{A2}} \Phi_{kji,\alpha\beta}^\theta,$$

$$\Phi_{ikj,\alpha\beta}^\theta = 0 \text{ if } N_{ikj} = 0,$$

$$\det[\Phi_{kji,\alpha\beta}^\theta] \neq 0. \quad (4)$$

Conditions (4) form a set of non-linear equations with variables N_{ijk} , $F_{kln,\gamma\lambda}^{ijm,\alpha\beta}$, $P_i^{kj,\alpha\beta}$, A^i and $(\theta_F, \theta_{P1}, \theta_{P2}, \theta_{A1}, \theta_{A2})$, which are tensor labels for fixed points. Following the previous discussion, the solutions $(N_{ijk}, F_{kln,\gamma\lambda}^{ijm,\alpha\beta}, P_i^{kj,\alpha\beta}, A^i)$ will then give us a labeling of different topological orders.

After obtaining such a tensor labeling for the ground state wave function, the next natural questions to ask are: Are they in one-to-one correspondence with different topological orders? How can we physically understand these tensors? Are there any physical quantities that we can at least numerically measure?

In fact, the non-Abelian Berry's phases T and S (up to unitary transformations) provide an answer to the above questions. Not only can T and S give a one-to-one label for different topological orders, but they can also provide a link between the fixed-point ground states and their corresponding quasi-particle excitations. We believe that the description given by the T - and S -matrices is complete, meaning that they can completely characterize different non-chiral topological orders. Further calculations of various topological properties thus can all be obtained from T - and S -matrices.

Now we want to briefly introduce the concept of non-Abelian-Berry's-phase description of topological order which was first introduced in Ref. 8. The more detailed description will be given in the next section of the paper. The non-Abelian Berry's phases are obtained from two types of transformations named T- and S-transformation, both defined on a torus. The "T-transformation" can be defined by twisting a fixed-point graph along an axis (let us say the x -direction) by 360° ; whereas the "S-transformation" can be defined by rotating a fixed-point graph by 90° . Essentially they are all discrete deformations of a fixed-point graph on a torus. As hinted from the one-to-one correspondence between the ground state degeneracy on a torus and the number of different types of quasi-particles, the information of the quasi-particles is always encoded in the geometry of the torus. Here again, through the non-Abelian Berry's phases of the ground states, we can "decode" the information about their quasi-particles. So T - and S -matrices give a better description of topological orders. In this paper, we will label different topological orders by their resulting T and S -matrices.

Also mathematically, the relationship between T - and S -matrix labels and fixed-point-tensor labels can be understood within tensor category theory. On one hand, the T - and S -matrices describe a set quasiparticle excitations, which may have fractional and/or non-Abelian statistics and are described by a modular tensor category \mathcal{T} . On the other hand, the fixed-point tensors correspond to the many-body wave functions of exact topological orders, which are described by unitary fusion category \mathcal{F} . Thus to calculate the T - and S -matrices from the fixed-point tensors is to calculate the quasiparticle excitations from the many-body wave functions, which corresponds to calculating the modular tensor category \mathcal{T} from a uni-

tary fusion category \mathcal{F} . Mathematically, calculating \mathcal{T} from \mathcal{F} corresponds to taking the "Drinfeld center" of the unitary fusion category \mathcal{F} . Our calculation of T - and S -matrices from the fixed-point tensors corresponds exactly to taking the "Drinfeld center" of the unitary fusion category \mathcal{F} .

This picture agrees perfectly with our calculations: we perform modular transformations on several fixed-point states (III A, III B, III C, III E, III F), all having the structure of unitary tensor category; our resulting T - and S -matrices for the quasi-particle excitations are all of the structure of modular tensor category. This result further strengthened our belief that tensor category theory is the mathematical structure behind topological order.

In this paper, we present many fixed-point solutions to eqn. (4), representing many exact topological orders. We then apply "modular transformations" to many of the obtained results (III A, III B, III C, III E, III F) to get their T and S -matrices, describing their corresponding quasi-particles.

Note that there's a special solution, *ie* the "chiral" case III H. In that case, the labeling fixed-point tensors form the so-called "multi-fusion category" and its fusion rule breaks the "chiral" symmetry. Although the resulting fixed-point wave function has a trivial topological order without any symmetry, we anticipate that the "chiral" case can be highly non-trivial after introducing certain symmetries.

III. LIST OF DIFFERENT TOPOLOGICAL ORDERS

In this section, we present a list of all fixed-point solutions obtained so far from solving eqn. (4). The solutions consist of fixed-point gLU transformations ($N_{ijk}, F_{kln, \alpha\beta}^{ijm}, P_i^{kj, \alpha\beta}$) and fixed-point wave functions A^i . For most of the cases (III A, III B, III C, III E, III F), we also present their corresponding T and S -matrices from modular transformations.

A. $N = 1$ loop states – the \mathbb{Z}_2 states

Let us first consider a system where there are only two states $|0\rangle$ and $|1\rangle$ on each link of the graph. We choose $i^* = i$ and the simplest fusion rule that satisfies eqn. (4) (we call the N tensors satisfying eqn. (4) as "fusion rule"):

$$\begin{aligned} N_{000} &= N_{110} = N_{101} = N_{011} = 1, \\ \text{other } N_{ijk} &= 0. \end{aligned} \quad (5)$$

Since $N_{ijk} \leq 1$, there are no states on the vertices. So the indices α, β, \dots labeling the states on a vertex can be suppressed.

The above fusion rule corresponds to the fusion rule of the $N = 1$ loop states discussed in Ref. 12, thus the

name $N = 1$ loop states. Note further that the three edge labels of N also form a \mathbb{Z}_2 group: for example, $N_{110} = 1$ represents the group action $1 \otimes 1 = 0$ (Here our group action is addition). Thus we call the states obtained in this section the \mathbb{Z}_2 states.

Due to relation eqn. (4), different components of tensor F_{kln}^{ijm} are not independent. There are only four independent potentially non-zero components, denoted as f_0, \dots, f_3 :

$$\begin{aligned} F_{000}^{000} &= f_0 \\ F_{111}^{000} &= (F_{100}^{011} \text{ graph})^* = (F_{010}^{101} \text{ graph})^* \\ &= F_{001}^{110} \text{ graph} = f_1 \\ F_{011}^{011} &= (F_{101}^{101} \text{ graph})^* = f_2 \\ F_{110}^{110} &= f_3 \end{aligned} \quad (6)$$

We note that F_{kln}^{ijm} in eqn. (2) relates wave functions on two graphs. In the above we have drawn the two related graphs right after the F tensor. The first graph following F corresponds to the graph on the left-hand side of eqn. (2) and the second one corresponds to the graph on the right-hand side of eqn. (2). The dotted line corresponds to the $|0\rangle$ -state on the link and the solid line corresponds to the $|1\rangle$ -state on the link. There are four potentially non-zero components in P_i^{kj} , which are denoted by p_0, \dots, p_3 :

$$P_0^{00} = p_0, \quad P_0^{01} = p_1, \quad P_1^{00} = p_2, \quad P_1^{01} = p_3. \quad (7)$$

We can adjust the total phases of p_i and A^i to make $p_0 \geq 0$ and $A^0 \geq 0$. We can also use a gauge transformation to make $f_1 \geq 0$.

The fixed-point conditions (4) form a set of non-linear equations on the ten variables f_i, p_i , and A^i . Many of the non-linear equations are dependent or even equivalent. Using a computer algebraic system, we simplify the set of non-linear equations. The simplified equations are (after making the phase choice described above)

$$\begin{aligned} f_0 &= f_1 = f_2 = 1, \quad f_3 = \eta, \\ p_1 &= p_3 = \eta p_0, \quad p_2 = p_0, \\ p_0^2 + |p_1|^2 &= 1, \quad |p_2|^2 + |p_3|^2 = 1, \\ p_1 A^0 &= p_2 A^1, \quad \eta p_3 A^1 = p_1 A^0, \quad |A^0|^2 + |A^1|^2 = 1 \end{aligned} \quad (8)$$

where $\eta = \pm 1$. The above simplified equations can be solved exactly. We find two isolated solutions parameterized by $\eta = \pm 1$:

$$\begin{aligned} f_0 &= f_1 = f_2 = 1, \quad f_3 = \eta, \\ p_0 &= p_2 = \frac{1}{\sqrt{2}}, \quad p_1 = p_3 = \frac{\eta}{\sqrt{2}}, \\ A^0 &= \frac{1}{\sqrt{2}}, \quad A^1 = \frac{\eta}{\sqrt{2}}. \end{aligned} \quad (9)$$

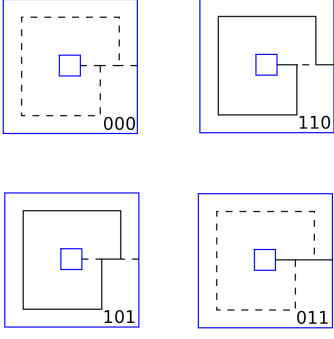


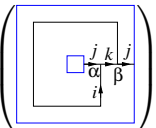
FIG. 1: (Color online) The 4 characteristic non-contractable graphs on a torus. (The inner square and the outer square are the physical boundary of a torus.) Any other fixed-point graphs can always be reduced to the above four by F-moves and P-moves, but the four types cannot be changed into each other. The dotted line represents the $|0\rangle$ -state on the edges, and the solid line represents the $|1\rangle$ -state on the edges. The three integers ijk at the lower right corner of each graph are the edge labels following the convention of eqn. (11).

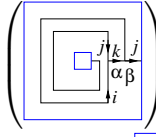
We also find

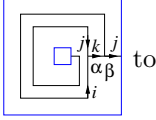
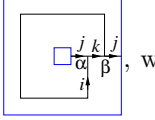
$$e^{i\theta_F} = e^{i\theta_{P1}} = e^{i\theta_{P2}} = e^{i\theta_{A1}} = e^{i\theta_{A2}} = 1. \quad (10)$$

The above solutions ($F_{kl\eta, \gamma\lambda}^{ijm, \alpha\beta}$, $P_i^{kj, \alpha\beta}$, A^i) with $\eta = \pm 1$ both correspond to fixed-point states. The $\eta = 1$ state is an equal weight superposition of all the graphic states that satisfy the fusion rule, whereas the $\eta = -1$ state is also a superposition of all fusion-rule-satisfying graphic states, but some with coefficient 1 and some others with coefficient -1 .

Having obtained the abstract fixed-point solutions, we now want to physically understand the results by introducing the concept of “modular transformations”. Modular transformations are defined on a torus (*ie* a planar graph with periodic boundary conditions in both x - and y -directions). Notice that after putting the above states onto a torus, there will be four different types of non-contractable graphs (see Fig. 1). They correspond to four types of fixed-point states that are linearly independent (meaning they cannot be transformed into each other through F or P -moves) and form the degenerate ground-state subspace of a local Hamiltonian (See Appendix A for the form of the Hamiltonian). The modular transformations can be defined within this ground-state subspace. We will first introduce the “ T -transformation”, also known as the method of Dehn twist. As in Ref. 14, we define the Dehn twist formally by requiring it to map a fixed-point state $\Phi_{\text{fix}}^{\alpha\beta}(i, j, k, \alpha, \beta) =$

$\Phi_{\text{fix}}^{\alpha\beta}$  on a torus to another fixed-point state defined on a different graph $\tilde{\Phi}_{\text{fix}}^{\alpha\beta}(i, j, k, \alpha, \beta) =$

$\tilde{\Phi}_{\text{fix}}^{\alpha\beta}$ . Then we can use an F -move to de-

form the graph  to , which leads to

a unitary transformation T between the four fixed-point states on the torus, called the “ T -transformation”. The deformation process could be seen more clearly from the following:

$$\begin{aligned} & \Phi_{\text{fix}}^{\alpha\beta} \left(\text{Diagram 101} \right) \xrightarrow{\text{Dehn twist}} \Phi_{\text{fix}}^{\alpha\beta} \left(\text{Diagram 000} \right) \\ &= \sum_{l, \chi\delta} F_{i^* j l^*, \chi\delta}^{ijk, \alpha\beta} \Phi_{\text{fix}}^{\chi\delta} \left(\text{Diagram with } \chi, \delta \right) \quad (F\text{-move}) \\ &= \sum_{l, \chi\delta} F_{i^* j l^*, \chi\delta}^{ijk, \alpha\beta} \Phi_{\text{fix}}^{\chi\delta} \left(\text{Diagram with } i, j, l, \chi, \delta \right) \quad (\text{Deformation}) \\ &= \sum_l F_{i^* j l^*}^{ijk} \Phi_{\text{fix}} \left(\text{Diagram 101} \right). \quad (11) \end{aligned}$$

In the last step above, we have suppressed the vertex indices $\alpha, \beta, \delta, \chi$ because a maximum of one state is allowed on each vertex.

Writing “ T -transformation” in the basis of the four non-contractable fixed point states on the torus, we get a 4 by 4 unitary matrix with elements $F_{i^* j l^*}^{ijk}$. This matrix is called as “ T -matrix”. The basis of the 4 by 4 matrix is defined as follows:

$$\Phi_{\text{fix}} \left(\text{Diagram 000} \right) = (1, 0, 0, 0),$$

$$\Phi_{\text{fix}} \left(\text{Diagram 101} \right) = (0, 1, 0, 0),$$

$$\Phi_{\text{fix}} \left(\text{Diagram 011} \right) = (0, 0, 1, 0),$$

When $\eta = 1$, we have:

$$T = \begin{pmatrix} 1 & 0 & 0 & 0 \\ 0 & 1 & 0 & 0 \\ 0 & 0 & 0 & 1 \\ 0 & 0 & 1 & 0 \end{pmatrix} \quad (15)$$

$$S = \begin{pmatrix} 1 & 0 & 0 & 0 \\ 0 & 0 & 1 & 0 \\ 0 & 1 & 0 & 0 \\ 0 & 0 & 0 & 1 \end{pmatrix} \quad (16)$$

We can choose a new basis to make the T and S -matrices be in a more standard form. In this new basis, we require that the T -matrix to be diagonalized and at the same time, S -matrix to satisfy the following requirements:?

1. $N_{ij}^k = \sum_n \frac{S_{n,i} S_{n,j} S_{n,k}^*}{S_{n,1}}$ is a non-negative integer,
2. $S_{i,j} = S_{j,i}$,
3. $S_{1,i} > 0$,
4. $S^2 = C$, $C^2 = 1$, $C|i\rangle = |i^*\rangle$, (17)
5. $e^{i \sum_j A_{ij} \theta_j} = e^{i \frac{4}{3} \sum_j A_{ij} \theta_j}$, $A_{ij} = 2N_{ii^*}^j N_{ij}^i + N_{ii}^j N_{j i^*}^i$,

where C generates a permutation of the basis, $C|i\rangle = |i^*\rangle$, that satisfy $i^{**} = i$, and $e^{i\theta_i}$ is the i^{th} eigenvalue of T . It is conjectured that the T and S -matrices satisfying the above requirements are unique (up to permutations of the basis), and thus the basis of T and S -matrices are completely fixed through the above requirements (up to permutations.) Numerical simulations have been done in several cases in the later sections of the paper, all agreeing with the conjecture.

In the above, $S_{i,j}$ represents the (i,j) -th matrix element of the S -matrix, and $S_{i,j}^*$ is its complex conjugate. In Modular Tensor Category theory, these are precisely the conditions satisfied by the “modular matrix” S and the “diagonal twist” matrix T ; thus the name for our T and S -matrix. The first condition above is the so-called Verlinde Formula; it gives the fusion rule for the quasi-particle excitations. (Note that this is different from the fusion rule 5, which is the fusion rule for fixed-point ground states.)

Now, diagonalize the T -matrix and make the S -matrix satisfy 17, we have:

$$T = \begin{pmatrix} 1 & 0 & 0 & 0 \\ 0 & 1 & 0 & 0 \\ 0 & 0 & 1 & 0 \\ 0 & 0 & 0 & -1 \end{pmatrix} \quad (18)$$

$$S = \frac{1}{2} \begin{pmatrix} 1 & 1 & 1 & 1 \\ 1 & 1 & -1 & -1 \\ 1 & -1 & 1 & -1 \\ 1 & -1 & -1 & 1 \end{pmatrix} \quad (19)$$

Numerical simulations show that the above T and S -matrices are unique (up to permutation of basis.) The above T and S -matrices match exactly with the corresponding matrices in the “Toric Code modular tensor category” in Ref. 15. From the dimension of the T and S -matrices, we can see that there are four different types of quasi-particles. From calculating eqn. (17), we can get the fusion rules between the quasi-particle excitations. The quasi-particle statistical angles are given by the eigenvalues of T -matrix.^{8,16} The quantum dimensions of these four quasi-particles are given by the first row (column) of the S -matrix.

Note that the $K = \begin{pmatrix} 0 & 2 \\ 2 & 0 \end{pmatrix} U(1) \times U(1)$ Chern-Simons (CS) theory also has 4 types of quasiparticles with statistical angles

$$(e^{i\theta_i}) = (1, 1, 1, -1).$$

Therefore, the $\eta = 1 \mathbb{Z}_2$ state can be described by the above CS theory.

When $\eta = -1$, we have:

$$T = \begin{pmatrix} 1 & 0 & 0 & 0 \\ 0 & 1 & 0 & 0 \\ 0 & 0 & 0 & 1 \\ 0 & 0 & -1 & 0 \end{pmatrix} \quad (20)$$

$$S = \begin{pmatrix} 1 & 0 & 0 & 0 \\ 0 & 0 & 1 & 0 \\ 0 & 1 & 0 & 0 \\ 0 & 0 & 0 & -1 \end{pmatrix} \quad (21)$$

Again, we can diagonalize the T -matrix and make the S -matrix satisfy 17 under a proper basis; numerical simulations show that such a basis is unique (up to permutations). In such a basis, we have:

$$T = \begin{pmatrix} 1 & 0 & 0 & 0 \\ 0 & -i & 0 & 0 \\ 0 & 0 & i & 0 \\ 0 & 0 & 0 & 1 \end{pmatrix} \quad (22)$$

$$S = \frac{1}{2} \begin{pmatrix} 1 & 1 & 1 & 1 \\ 1 & -1 & 1 & -1 \\ 1 & 1 & -1 & -1 \\ 1 & -1 & -1 & 1 \end{pmatrix} \quad (23)$$

In this particular case, the above T and S matrices can be further reduced to the following forms:

$$T = \begin{pmatrix} 1 & 0 \\ 0 & i \end{pmatrix} \otimes \begin{pmatrix} 1 & 0 \\ 0 & -i \end{pmatrix} \quad (24)$$

$$S = \frac{1}{\sqrt{2}} \begin{pmatrix} 1 & 1 \\ 1 & -1 \end{pmatrix} \otimes \frac{1}{\sqrt{2}} \begin{pmatrix} 1 & 1 \\ 1 & -1 \end{pmatrix} \quad (25)$$

which shows the “doubled” structure of the quasi-particles. The above T and S -matrices match exactly with the “doubled Semion” modular tensor category in Ref. 15. Again, we can see that there are four different types of quasi-particles from the dimension of the T and S -matrices. From calculating eqn. (17), we can get the fusion rules between the quasi-particle excitations. The quasi-particle statistics are given by the eigenvalues of T -matrix, whereas the quantum dimensions of different quasi-particles are given by the elements on the first row of S -matrix.

Notice that the eigenvalues of T -matrix again match with the $K = \begin{pmatrix} 0 & 2 \\ 2 & 2 \end{pmatrix}$ CS theory (which is equivalent to the $K = \begin{pmatrix} 2 & 0 \\ 0 & -2 \end{pmatrix}$ CS theory), which has 4 types of quasiparticles with statistical angles

$$(e^{i\theta_i}) = (1, 1, i, -i).$$

Also, the “doubled” structure hints that the effective theory can be “decoupled”, which is exactly what we get here: $K = \begin{pmatrix} 2 & 0 \\ 0 & -2 \end{pmatrix}$ can indeed be decoupled. Therefore, the $\eta = -1 \mathbb{Z}_2$ state can be described by the $K = \begin{pmatrix} 0 & 2 \\ 2 & 2 \end{pmatrix}$ CS theory.

B. $N = 1$ string-net state – the “Fibonacci” state

To obtain another class of simple solutions, we modify the fusion rule to

$$\begin{aligned} N_{000} = N_{110} = N_{101} = N_{011} = N_{111} = 1, \\ \text{other } N_{ijk} = 0. \end{aligned} \quad (26)$$

while keeping everything the same. The above N_{ijk} also satisfies eqn. (4).

The new fusion rule corresponds to the fusion rule for the $N = 1$ string-net state discussed in Ref. 12, thus the name $N = 1$ string-net state. Notice the additional fusion rule can be written as $1 \otimes 1 = 0 \oplus 1$ which looks like Fibonacci’s golden rule, we also refer to the state as the “Fibonacci State”.

Again, due to the relation eqn. (4), the different components of the tensor F_{klm}^{ijm} are not independent. Now there are seven independent potentially non-zero compo-

nents which are denoted as f_0, \dots, f_6 :

$$\begin{aligned} F_{000}^{000} &= f_0 \\ F_{111}^{000} &= (F_{100}^{011})^* = (F_{010}^{101})^* \\ &= F_{001}^{110} = f_1 \\ F_{011}^{011} &= (F_{101}^{101})^* = f_2 \\ F_{111}^{011} &= (F_{111}^{101})^* = F_{011}^{111} \\ &= (F_{101}^{111})^* = f_3 \\ F_{110}^{110} &= f_4 \\ F_{111}^{110} &= (F_{110}^{111})^* = f_5 \\ F_{111}^{111} &= f_6 \end{aligned} \quad (27)$$

Note that F ’s described by f_1 and f_5 are the only F ’s that change the number of $|1\rangle$ -links and the number of $|1\rangle|1\rangle|1\rangle$ -vertices. So we can use the local unitary transformation $e^{i(\theta\hat{M}_1 + \phi\hat{M}_{111})}$ to make f_1 and f_5 to be positive real numbers. (Here \hat{M}_1 is the total number of $|1\rangle$ -links and \hat{M}_{111} is the total number of $|1\rangle|1\rangle|1\rangle$ -vertices.) We also use the freedom of adjusting the total sign of F_{klm}^{ijm} to make $\text{Re}(f_0) \geq 0$.

There are five potentially non-zero components in P_i^{kj} , which are denoted by p_0, \dots, p_4 :

$$\begin{aligned} P_0^{00} = p_0, \quad P_0^{01} = p_1, \quad P_1^{00} = p_2, \\ P_1^{01} = p_3, \quad P_1^{11} = p_4. \end{aligned} \quad (28)$$

We use the freedom of adjusting the total phase of P_i^{kj} to make p_0 to be a positive number. We can also use the freedom of adjusting the total phase of A^i to make A^0 to be a positive number.

The fixed-point conditions (eqn. (4)) form a set of non-linear equations on the variables f_i, p_i , and A^i , which can be simplified. The simplified equations have the following form

$$\begin{aligned} f_0 = f_1 = f_2 = f_3 = 1, \quad f_4 = f_5^2 = -f_6 > 0, \\ p_1^2 f_4^2 + p_1^2 = 1, \quad p_0 = f_4 p_1, \quad p_2 = p_0, \quad p_3 = p_1, \quad p_4 = 0 \\ A^0 = f_4 A^1, \quad (A^0)^2 + (A^1)^2 = 1, \quad f_4^2 + f_4 - 1 = 0. \end{aligned} \quad (29)$$

Let γ be the positive solution of $\gamma^2 + \gamma = 1$: $\gamma = \frac{\sqrt{5}-1}{2}$. We see that $f_5 = \sqrt{\gamma}$. The above can be written as

$$\begin{aligned} f_0 = f_1 = f_2 = f_3 = 1, \quad f_4 = -f_6 = \gamma, \quad f_5 = \sqrt{\gamma}, \\ p_0 = p_2 = \frac{\gamma}{\sqrt{\gamma^2 + 1}}, \quad p_1 = p_3 = \frac{1}{\sqrt{\gamma^2 + 1}}, \quad p_4 = 0, \\ A^0 = \frac{\gamma}{\sqrt{\gamma^2 + 1}}, \quad A^1 = \frac{1}{\sqrt{\gamma^2 + 1}}. \end{aligned} \quad (30)$$

We also find

$$e^{i\theta_F} = e^{i\theta_{P1}} = e^{i\theta_{P2}} = e^{i\theta_{A1}} = e^{i\theta_{A2}} = 1. \quad (31)$$

The fixed-point state above corresponds to the $N = 1$ string-net condensed state¹².

Following the logic from last section, we will now apply the modular transformations. Let us first consider Dehn twist on a torus. Note that we now formally have 5 possible non-contractable graphs on a torus rather than 4, due to the additional fusion rule. (Recall Fig. 1; the additional graph would be a graph with all solid lines.) Doing the Dehn twist for all 5 graphic states using (11), we have:

$$\Phi_{\text{fix}} \left(\begin{array}{c} \text{Diagram 1} \\ \text{000} \end{array} \right) = F_{000}^{000} \Phi_{\text{fix}} \left(\begin{array}{c} \text{Diagram 2} \\ \text{000} \end{array} \right)$$

$$\Phi_{\text{fix}} \left(\begin{array}{c} \text{Diagram 3} \\ \text{110} \end{array} \right) = F_{110}^{110} \Phi_{\text{fix}} \left(\begin{array}{c} \text{Diagram 4} \\ \text{011} \end{array} \right) \\ + F_{111}^{110} \Phi_{\text{fix}} \left(\begin{array}{c} \text{Diagram 5} \\ \text{111} \end{array} \right)$$

$$\Phi_{\text{fix}} \left(\begin{array}{c} \text{Diagram 6} \\ \text{101} \end{array} \right) = F_{101}^{101} \Phi_{\text{fix}} \left(\begin{array}{c} \text{Diagram 7} \\ \text{101} \end{array} \right)$$

$$\Phi_{\text{fix}} \left(\begin{array}{c} \text{Diagram 8} \\ \text{011} \end{array} \right) = F_{011}^{011} \Phi_{\text{fix}} \left(\begin{array}{c} \text{Diagram 9} \\ \text{110} \end{array} \right)$$

$$\Phi_{\text{fix}} \left(\begin{array}{c} \text{Diagram 10} \\ \text{111} \end{array} \right) = F_{110}^{111} \Phi_{\text{fix}} \left(\begin{array}{c} \text{Diagram 11} \\ \text{011} \end{array} \right) \\ + F_{111}^{111} \Phi_{\text{fix}} \left(\begin{array}{c} \text{Diagram 12} \\ \text{111} \end{array} \right)$$

We thus obtain the 5 by 5 T -matrix for the Fibonacci state as follows:

$$T = \begin{pmatrix} F_{000}^{000} & 0 & 0 & 0 & 0 \\ 0 & 0 & 0 & F_{011}^{011} & 0 \\ 0 & 0 & F_{101}^{101} & 0 & 0 \\ 0 & F_{110}^{110} & 0 & 0 & F_{110}^{111} \\ 0 & F_{111}^{110} & 0 & 0 & F_{111}^{111} \end{pmatrix} \quad (32)$$

Similarly, we can also get the S -matrix by applying 90° rotations to all five non-contractable states on a torus:

$$\Phi_{\text{fix}} \left(\begin{array}{c} \text{Diagram 13} \\ \text{000} \end{array} \right) = F_{000}^{000} \Phi_{\text{fix}} \left(\begin{array}{c} \text{Diagram 14} \\ \text{000} \end{array} \right)$$

$$\Phi_{\text{fix}} \left(\begin{array}{c} \text{Diagram 15} \\ \text{110} \end{array} \right) = F_{110}^{110} \Phi_{\text{fix}} \left(\begin{array}{c} \text{Diagram 16} \\ \text{110} \end{array} \right) \\ + F_{111}^{110} \Phi_{\text{fix}} \left(\begin{array}{c} \text{Diagram 17} \\ \text{111} \end{array} \right)$$

$$\Phi_{\text{fix}} \left(\begin{array}{c} \text{Diagram 18} \\ \text{101} \end{array} \right) = F_{101}^{101} \Phi_{\text{fix}} \left(\begin{array}{c} \text{Diagram 19} \\ \text{011} \end{array} \right)$$

$$\Phi_{\text{fix}} \left(\begin{array}{c} \text{Diagram 20} \\ \text{011} \end{array} \right) = F_{011}^{011} \Phi_{\text{fix}} \left(\begin{array}{c} \text{Diagram 21} \\ \text{101} \end{array} \right)$$

$$\Phi_{\text{fix}} \left(\begin{array}{c} \text{Diagram 22} \\ \text{111} \end{array} \right) = F_{110}^{111} \Phi_{\text{fix}} \left(\begin{array}{c} \text{Diagram 23} \\ \text{110} \end{array} \right) \\ + F_{111}^{111} \Phi_{\text{fix}} \left(\begin{array}{c} \text{Diagram 24} \\ \text{111} \end{array} \right)$$

From which we can get the 5 by 5 S -matrix for the Fibonacci state:

$$S = \begin{pmatrix} F_{000}^{000} & 0 & 0 & 0 & 0 \\ 0 & F_{110}^{110} & 0 & 0 & F_{110}^{111} \\ 0 & 0 & 0 & F_{011}^{011} & 0 \\ 0 & 0 & F_{101}^{101} & 0 & 0 \\ 0 & F_{111}^{110} & 0 & 0 & F_{111}^{111} \end{pmatrix} \quad (33)$$

Now we can substitute in the values of the F tensors, and thus obtain:

$$T = \begin{pmatrix} 1 & 0 & 0 & 0 & 0 \\ 0 & 0 & 0 & 1 & 0 \\ 0 & 0 & 1 & 0 & 0 \\ 0 & \gamma & 0 & 0 & \sqrt{\gamma} \\ 0 & \sqrt{\gamma} & 0 & 0 & -\gamma \end{pmatrix} \quad (34)$$

$$S = \begin{pmatrix} 1 & 0 & 0 & 0 & 0 \\ 0 & \gamma & 0 & 0 & \sqrt{\gamma} \\ 0 & 0 & 0 & 1 & 0 \\ 0 & 0 & 1 & 0 & 0 \\ 0 & \sqrt{\gamma} & 0 & 0 & -\gamma \end{pmatrix} \quad (35)$$

where $\gamma = \frac{\sqrt{5}-1}{2}$.

There is, however, a small complication here compared to the previous \mathbb{Z}_2 case. Although there are now five possible non-contractable graphs on a torus, they are no longer linearly independent (meaning they can be transformed into each other through F or P -moves) and are not all fixed-point graphs. Thus they don't all correspond to ground states of a local Hamiltonian. As can be checked using the Hamiltonian construction in Appendix A, the ground state subspace in this case is only 4-fold degenerate. We thus need to restrict our modular transformations to be within this ground state subspace. In order to get the T and S -matrix within the ground states, we need to project the above obtained matrices onto its 4×4 ground-state subspace. Such a process can be easily done by diagonalizing the Hamiltonian and projecting the T and S -matrices only to the ground-state subspace; see Appendix A for details.

After the projection, we can again diagonalize the T -matrix and make the S -matrix satisfy 17 under a proper basis; numerical simulations again show that such a basis is unique (up to permutations). We thus have the final form of T and S :

$$T = \begin{pmatrix} 1 & 0 & 0 & 0 \\ 0 & e^{i\frac{4\pi}{5}} & 0 & 0 \\ 0 & 0 & e^{-i\frac{4\pi}{5}} & 0 \\ 0 & 0 & 0 & 1 \end{pmatrix} \quad (36)$$

$$S = \frac{5 - \sqrt{5}}{10} \begin{pmatrix} 1 & \frac{1+\sqrt{5}}{2} & \frac{1+\sqrt{5}}{2} & \frac{3+\sqrt{5}}{2} \\ \frac{1+\sqrt{5}}{2} & -1 & \frac{3+\sqrt{5}}{2} & \frac{-1-\sqrt{5}}{2} \\ \frac{1+\sqrt{5}}{2} & \frac{3+\sqrt{5}}{2} & -1 & \frac{-1-\sqrt{5}}{2} \\ \frac{3+\sqrt{5}}{2} & \frac{-1-\sqrt{5}}{2} & \frac{-1-\sqrt{5}}{2} & 1 \end{pmatrix} \quad (37)$$

As can be easily seen, the above S -matrix is real and symmetric. Also in this particular case, the above T and S matrices can be further reduced to the following forms:

$$T = \begin{pmatrix} 1 & 0 \\ 0 & e^{-i\frac{4\pi}{5}} \end{pmatrix} \otimes \begin{pmatrix} 1 & 0 \\ 0 & e^{i\frac{4\pi}{5}} \end{pmatrix} \quad (38)$$

$$S = \frac{5 - \sqrt{5}}{10} \begin{pmatrix} 1 & \frac{1+\sqrt{5}}{2} \\ \frac{1+\sqrt{5}}{2} & -1 \end{pmatrix} \otimes \begin{pmatrix} 1 & \frac{1+\sqrt{5}}{2} \\ \frac{1+\sqrt{5}}{2} & -1 \end{pmatrix} \quad (39)$$

which shows the ‘‘doubled’’ structure of the quasi-particles. The above T and S -matrices match exactly with the doubled ‘‘Fibonacci’’ modular tensor category in Ref. 15. As before, we can tell there are four different types of quasi-particles from the dimension of T and S ; we can also get the fusion rules between quasi-particle excitations from calculating eqn. (17). The quasi-particle statistical angles are given by the eigenvalues of T , whereas the quantum dimensions of different quasi-particles are given by the first row (column) of the S -matrix.

Following the last section, here we want to also comment on the eigenvalues of T -matrix. These eigenvalues

correspond exactly to the quasiparticle statistical angles of the doubled $SO(3)$ Chern-Simons gauge theory:

$$(e^{i\theta_i}) = (1, 1, e^{i\frac{4\pi}{5}}, e^{-i\frac{4\pi}{5}}).$$

Thus the ‘‘Fibonacci’’ state can be described by the doubled $SO(3)$ CS theory.

C. An $N = 2$ string-net state – the ‘‘Pfaffian’’ state

Here we will give a more complicated example of a non-orientable string-net state. We choose $N = 2$, $0^* = 0$, $1^* = 1$, $2^* = 2$, and

$$\begin{aligned} N_{000} &= N_{011} = N_{110} = N_{101} = N_{022} = N_{202} = N_{220} \\ &= N_{112} = N_{121} = N_{211} = 1. \end{aligned} \quad (40)$$

The above N_{ijk} satisfies eqn. (4).

Similar to the \mathbb{Z}_2 case, the three edge states of N form a structure called a ‘‘tensor category’’ with the following fusion rules between its three elements: $1 \otimes \sigma = \sigma$, $1 \otimes \psi = \psi$, $\psi \otimes \psi = 1$, $\sigma \otimes \sigma = 1 \oplus \psi$. In the above fusion rules, ‘‘1’’ represents state 0 on the edge, ‘‘ σ ’’ represents state 1 and ‘‘ ψ ’’ represents state 2. (For example, N_{112} corresponds to $\sigma \otimes \sigma = \psi$.) Since the state also corresponds to the ‘‘Pfaffian’’ state in the Ising model, we have the name – ‘‘Pfaffian state’’.

Due to relation eqn. (4), different components of the tensor F_{klm}^{ijm} are not independent. There are fourteen independent potentially non-zero components which are denoted as f_0, \dots, f_{13} :

$$\begin{aligned} F_{000}^{000} &= f_0 \\ F_{111}^{000} &= (F_{100}^{011})^* = (F_{010}^{101})^* \\ &= F_{001}^{110} = f_1 \\ F_{222}^{000} &= (F_{200}^{022})^* = (F_{020}^{202})^* \\ &= F_{002}^{220} = f_2 \\ F_{011}^{011} &= (F_{101}^{101})^* = f_3 \\ F_{122}^{011} &= (F_{201}^{112})^* = F_{012}^{121} \\ &= (F_{111}^{202})^* = f_4 \end{aligned}$$

$$\begin{aligned}
F_{211}^{011} \langle \text{graph} \rangle &= (F_{121}^{101} \langle \text{graph} \rangle)^* = (F_{101}^{121} \langle \text{graph} \rangle)^* \\
&= F_{011}^{211} \langle \text{graph} \rangle = f_5 \\
F_{022}^{022} \langle \text{graph} \rangle &= (F_{202}^{202} \langle \text{graph} \rangle)^* = f_6 \\
F_{111}^{022} \langle \text{graph} \rangle &= (F_{212}^{101} \langle \text{graph} \rangle)^* = F_{021}^{112} \langle \text{graph} \rangle \\
&= (F_{102}^{211} \langle \text{graph} \rangle)^* = f_7 \\
F_{110}^{110} \langle \text{graph} \rangle &= f_8 \\
F_{112}^{110} \langle \text{graph} \rangle &= (F_{110}^{112} \langle \text{graph} \rangle)^* = f_9 \\
F_{112}^{112} \langle \text{graph} \rangle &= f_{10} \\
F_{221}^{110} \langle \text{graph} \rangle &= (F_{210}^{121} \langle \text{graph} \rangle)^* = (F_{120}^{211} \langle \text{graph} \rangle)^* \\
&= F_{111}^{220} \langle \text{graph} \rangle = f_{11} \\
F_{121}^{121} \langle \text{graph} \rangle &= (F_{211}^{211} \langle \text{graph} \rangle)^* = f_{12} \\
F_{220}^{220} \langle \text{graph} \rangle &= f_{13} \tag{41}
\end{aligned}$$

There are ten potentially non-zero components in P_i^{kj} , which are denoted by p_0, \dots, p_9 :

$$\begin{aligned}
P_0^{00} = p_0, \quad P_1^{01} = p_1, \quad P_0^{02} = p_2, \quad P_1^{00} = p_3, \quad P_1^{01} = p_4, \\
P_1^{21} = p_5, \quad P_1^{02} = p_6, \quad P_2^{00} = p_7, \quad P_2^{01} = p_8, \quad P_2^{02} = p_9. \tag{42}
\end{aligned}$$

Using the ‘‘gauge fixing’’ discussed in section Ref. 5, we can consistently fix the phases of $f_1, f_2, f_4, f_7, f_9, f_{11}, p_0$ and A^0 to make them positive. (Note that this ‘gauge fixing’ is non-trivial, since these phases are not completely independent; for e.g. the phases of f_4, f_7 are complex conjugates of each other.)

The fixed-point conditions (eqn. (4)) form a set of non-linear equations on the variables f_i, p_i , and A^i , which can be solved exactly. After applying the ‘gauge fixing’ discussed above, we find only one solution

$$\begin{aligned}
f_0 = f_1 = \dots = f_7 = f_{11} = f_{13} = 1, \\
f_8 = f_9 = -f_{10} = \frac{1}{\sqrt{2}}, \quad f_{12} = -1, \\
p_1 = p_4 = p_8 = \frac{1}{\sqrt{2}}, \quad p_5 = 0, \\
p_0 = p_2 = p_3 = p_6 = p_7 = p_9 = \frac{1}{2}, \\
A^0 = A^2 = \frac{1}{2}, \quad A^1 = \frac{1}{\sqrt{2}}. \tag{43}
\end{aligned}$$

We also find

$$e^{i\theta_F} = e^{i\theta_{P1}} = e^{i\theta_{P2}} = e^{i\theta_{A1}} = e^{i\theta_{A2}} = 1. \tag{44}$$

Now we are ready to apply the Modular transformations. First we try to get the T -matrix by applying the Dehn twists. In the ‘‘Pfaffian’’ case we have altogether 10 non-contractable graphs on a torus as can be seen in below. Applying Dehn twists to all of them using (11), we have:

$$\begin{aligned}
\Phi_{\text{fix}} \left(\begin{array}{c} \text{graph} \\ \text{000} \end{array} \right) &= F_{000}^{000} \Phi_{\text{fix}} \left(\begin{array}{c} \text{graph} \\ \text{000} \end{array} \right) \\
\Phi_{\text{fix}} \left(\begin{array}{c} \text{graph} \\ \text{110} \end{array} \right) &= F_{110}^{110} \Phi_{\text{fix}} \left(\begin{array}{c} \text{graph} \\ \text{011} \end{array} \right) \\
&\quad + F_{112}^{110} \Phi_{\text{fix}} \left(\begin{array}{c} \text{graph} \\ \text{211} \end{array} \right) \\
\Phi_{\text{fix}} \left(\begin{array}{c} \text{graph} \\ \text{220} \end{array} \right) &= F_{220}^{220} \Phi_{\text{fix}} \left(\begin{array}{c} \text{graph} \\ \text{022} \end{array} \right) \\
\Phi_{\text{fix}} \left(\begin{array}{c} \text{graph} \\ \text{101} \end{array} \right) &= F_{101}^{101} \Phi_{\text{fix}} \left(\begin{array}{c} \text{graph} \\ \text{101} \end{array} \right) \\
\Phi_{\text{fix}} \left(\begin{array}{c} \text{graph} \\ \text{011} \end{array} \right) &= F_{011}^{011} \Phi_{\text{fix}} \left(\begin{array}{c} \text{graph} \\ \text{110} \end{array} \right) \\
\Phi_{\text{fix}} \left(\begin{array}{c} \text{graph} \\ \text{211} \end{array} \right) &= F_{211}^{211} \Phi_{\text{fix}} \left(\begin{array}{c} \text{graph} \\ \text{112} \end{array} \right) \\
\Phi_{\text{fix}} \left(\begin{array}{c} \text{graph} \\ \text{121} \end{array} \right) &= F_{121}^{121} \Phi_{\text{fix}} \left(\begin{array}{c} \text{graph} \\ \text{121} \end{array} \right) \\
\Phi_{\text{fix}} \left(\begin{array}{c} \text{graph} \\ \text{202} \end{array} \right) &= F_{202}^{202} \Phi_{\text{fix}} \left(\begin{array}{c} \text{graph} \\ \text{202} \end{array} \right) \\
\Phi_{\text{fix}} \left(\begin{array}{c} \text{graph} \\ \text{112} \end{array} \right) &= F_{112}^{112} \Phi_{\text{fix}} \left(\begin{array}{c} \text{graph} \\ \text{211} \end{array} \right) \\
&\quad + F_{110}^{112} \Phi_{\text{fix}} \left(\begin{array}{c} \text{graph} \\ \text{011} \end{array} \right)
\end{aligned}$$

$$\Phi_{\text{fix}} \left(\begin{array}{c} \text{---} \\ \text{---} \\ \text{---} \\ \text{---} \\ \text{---} \\ \text{---} \\ \text{---} \\ \text{---} \\ \text{---} \\ \text{---} \end{array} \right) = F_{022}^{022} \Phi_{\text{fix}} \left(\begin{array}{c} \text{---} \\ \text{---} \\ \text{---} \\ \text{---} \\ \text{---} \\ \text{---} \\ \text{---} \\ \text{---} \\ \text{---} \\ \text{---} \end{array} \right)$$

We thus obtain the 10 by 10 T -matrix for the Pfaffian state:

$$T = \begin{pmatrix} 1 & 0 & 0 & 0 & 0 & 0 & 0 & 0 & 0 & 0 \\ 0 & 0 & 0 & 0 & 1 & 0 & 0 & 0 & 0 & 0 \\ 0 & 0 & 0 & 0 & 0 & 0 & 0 & 0 & 0 & 1 \\ 0 & 0 & 0 & 1 & 0 & 0 & 0 & 0 & 0 & 0 \\ 0 & \frac{1}{\sqrt{2}} & 0 & 0 & 0 & 0 & 0 & 0 & \frac{1}{\sqrt{2}} & 0 \\ 0 & \frac{1}{\sqrt{2}} & 0 & 0 & 0 & 0 & 0 & 0 & -\frac{1}{\sqrt{2}} & 0 \\ 0 & 0 & 0 & 0 & 0 & 0 & -1 & 0 & 0 & 0 \\ 0 & 0 & 0 & 0 & 0 & 0 & 0 & 1 & 0 & 0 \\ 0 & 0 & 0 & 0 & 0 & -1 & 0 & 0 & 0 & 0 \\ 0 & 0 & 1 & 0 & 0 & 0 & 0 & 0 & 0 & 0 \end{pmatrix} \quad (45)$$

Similarly, we can apply the 90° rotations and obtain the S -matrix. Without going into to much details, we give here the final result (under the same basis):

$$S = \begin{pmatrix} 1 & 0 & 0 & 0 & 0 & 0 & 0 & 0 & 0 & 0 \\ 0 & \frac{1}{\sqrt{2}} & 0 & 0 & 0 & 0 & 0 & 0 & \frac{1}{\sqrt{2}} & 0 \\ 0 & 0 & 1 & 0 & 0 & 0 & 0 & 0 & 0 & 0 \\ 0 & 0 & 0 & 0 & 1 & 0 & 0 & 0 & 0 & 0 \\ 0 & 0 & 0 & 1 & 0 & 0 & 0 & 0 & 0 & 0 \\ 0 & 0 & 0 & 0 & 0 & 0 & -1 & 0 & 0 & 0 \\ 0 & 0 & 0 & 0 & 0 & -1 & 0 & 0 & 0 & 0 \\ 0 & 0 & 0 & 0 & 0 & 0 & 0 & 0 & 0 & 1 \\ 0 & \frac{1}{\sqrt{2}} & 0 & 0 & 0 & 0 & 0 & 0 & -\frac{1}{\sqrt{2}} & 0 \\ 0 & 0 & 0 & 0 & 0 & 0 & 0 & 1 & 0 & 0 \end{pmatrix}. \quad (46)$$

As in the “Fibonacci” case, the above 10 non-contractable graphs are not all fixed-point graphs and do not all correspond to ground states of a local Hamiltonian. Using the Hamiltonian construction in Appendix A, it’s easy to check that the true ground state subspace is actually 9-fold; we can thus project the above matrices onto its ground state subspace. By carefully choosing the basis, we can again make the resulting 9×9 T -matrix diagonalized and the 9×9 S -matrix satisfy 17 at the same time, as shown below. Numerical simulations again show that such a basis is unique (up to permutations.)

$$T = \begin{pmatrix} 1 & 0 & 0 & 0 & 0 & 0 & 0 & 0 & 0 \\ 0 & e^{-i\frac{\pi}{8}} & 0 & 0 & 0 & 0 & 0 & 0 & 0 \\ 0 & 0 & -1 & 0 & 0 & 0 & 0 & 0 & 0 \\ 0 & 0 & 0 & e^{i\frac{\pi}{8}} & 0 & 0 & 0 & 0 & 0 \\ 0 & 0 & 0 & 0 & 1 & 0 & 0 & 0 & 0 \\ 0 & 0 & 0 & 0 & 0 & e^{-i\frac{7\pi}{8}} & 0 & 0 & 0 \\ 0 & 0 & 0 & 0 & 0 & 0 & -1 & 0 & 0 \\ 0 & 0 & 0 & 0 & 0 & 0 & 0 & e^{i\frac{7\pi}{8}} & 0 \\ 0 & 0 & 0 & 0 & 0 & 0 & 0 & 0 & 1 \end{pmatrix} \quad (47)$$

$$S = \frac{1}{4} \begin{pmatrix} 1 & \sqrt{2} & 1 & \sqrt{2} & 2 & \sqrt{2} & 1 & \sqrt{2} & 1 \\ \sqrt{2} & 0 & -\sqrt{2} & 2 & 0 & -2 & \sqrt{2} & 0 & -\sqrt{2} \\ 1 & -\sqrt{2} & 1 & \sqrt{2} & -2 & \sqrt{2} & 1 & -\sqrt{2} & 1 \\ \sqrt{2} & 2 & \sqrt{2} & 0 & 0 & 0 & -\sqrt{2} & -2 & -\sqrt{2} \\ 2 & 0 & -2 & 0 & 0 & 0 & -2 & 0 & 2 \\ \sqrt{2} & -2 & \sqrt{2} & 0 & 0 & 0 & -\sqrt{2} & 2 & -\sqrt{2} \\ 1 & \sqrt{2} & 1 & -\sqrt{2} & -2 & -\sqrt{2} & 1 & \sqrt{2} & 1 \\ \sqrt{2} & 0 & -\sqrt{2} & -2 & 0 & 2 & \sqrt{2} & 0 & -\sqrt{2} \\ 1 & -\sqrt{2} & 1 & -\sqrt{2} & 2 & -\sqrt{2} & 1 & -\sqrt{2} & 1 \end{pmatrix}. \quad (48)$$

The above S -matrix is again real and symmetric. Also in this particular case, the above T and S matrices can be further reduced to the following forms:

$$T = \begin{pmatrix} 1 & 0 & 0 \\ 0 & e^{i\frac{\pi}{8}} & 0 \\ 0 & 0 & -1 \end{pmatrix} \otimes \begin{pmatrix} 1 & 0 & 0 \\ 0 & e^{-i\frac{\pi}{8}} & 0 \\ 0 & 0 & -1 \end{pmatrix} \quad (49)$$

$$S = \frac{1}{2} \begin{pmatrix} 1 & \sqrt{2} & 1 \\ \sqrt{2} & 0 & -\sqrt{2} \\ 1 & -\sqrt{2} & 1 \end{pmatrix} \otimes \frac{1}{2} \begin{pmatrix} 1 & \sqrt{2} & 1 \\ \sqrt{2} & 0 & -\sqrt{2} \\ 1 & -\sqrt{2} & 1 \end{pmatrix} \quad (50)$$

which shows the “doubled” structure of the quasi-particles. The above T and S -matrices match exactly with the doubled “Ising” modular tensor category in Ref. 15. As before, we can tell that there are 9 types of different quasi-particles from the dimension of T and S and through calculating the Verlinde Formula 17, we can get the fusion rule between them. The quasi-particle statistics can be obtained from the eigenvalues of T -matrix and the quantum dimensions of these quasiparticles are given by the elements on the first row of S -matrix.

D. Another $N = 2$ string-net state – the S_3 state

By adding an additional fusion rule on top of the previous result, we can get yet another example of a non-orientable string-net state. Here we still choose $N = 2$, $0^* = 0$, $1^* = 1$, $2^* = 2$, and

$$\begin{aligned} N_{000} &= N_{011} = N_{110} = N_{101} = N_{022} = N_{202} = N_{220} \\ &= N_{111} = N_{112} = N_{121} = N_{211} = 1. \end{aligned} \quad (51)$$

The above N_{ijk} satisfies eqn. (4).

These fusion rules correspond to the $N = 2$ string-net model with non-orientable strings in Ref. 12. Following that paper, we will also call this state the S_3 state. As can be seen in the following, after gauge fixing, the fixed-point solutions completely agree with the “local rules” obtained in Ref. 12, thus we re-obtain another string-net state from local unitary transformation point of view. (Note that edge labels 1 and 2 are reversed in Ref. 12 compared to this paper.)

Due to relation eqn. (4), different components of the tensor F_{kln}^{ijm} are not independent. There are fourteen independent potentially non-zero components which are denoted as f_0, \dots, f_{18} :

$$\begin{aligned}
F_{000}^{000} &= f_0 \\
F_{111}^{000} &= (F_{100}^{011})^* = (F_{010}^{101})^* \\
&= F_{001}^{110} = f_1 \\
F_{222}^{000} &= (F_{200}^{022})^* = (F_{020}^{202})^* \\
&= F_{002}^{220} = f_2 \\
F_{011}^{011} &= (F_{101}^{101})^* = f_3 \\
F_{111}^{011} &= (F_{111}^{101})^* = F_{011}^{111} \\
&= (F_{101}^{111})^* = f_4 \\
F_{122}^{011} &= (F_{201}^{112})^* = F_{012}^{121} \\
&= (F_{111}^{202})^* = f_5
\end{aligned}$$

$$\begin{aligned}
F_{211}^{011} &= (F_{121}^{101})^* = (F_{101}^{121})^* \\
&= F_{011}^{211} = f_6 \\
F_{022}^{022} &= (F_{202}^{202})^* = f_7 \\
F_{111}^{022} &= (F_{212}^{101})^* = F_{021}^{112} \\
&= (F_{102}^{211})^* = f_8 \\
F_{110}^{110} &= f_9 \\
F_{111}^{110} &= (F_{111}^{111})^* = f_{10} \\
F_{112}^{110} &= (F_{110}^{112})^* = f_{11}
\end{aligned}$$

$$\begin{aligned}
F_{111}^{111} &= f_{12} \\
F_{112}^{111} &= (F_{111}^{112})^* = f_{13} \\
F_{112}^{112} &= f_{14} \\
F_{121}^{111} &= (F_{211}^{111})^* = F_{111}^{121} \\
&= (F_{111}^{211})^* = f_{15} \\
F_{221}^{110} &= (F_{210}^{121})^* = (F_{120}^{211})^* \\
&= F_{111}^{220} = f_{16} \\
F_{121}^{121} &= (F_{211}^{121})^* = f_{17} \\
F_{220}^{220} &= f_{18}
\end{aligned} \tag{52}$$

There are ten potentially non-zero components in P_i^{kj} , which are denoted by p_0, \dots, p_9 :

$$\begin{aligned}
P_0^{00} &= p_0, \quad P_0^{01} = p_1, \quad P_0^{02} = p_2, \quad P_1^{00} = p_3, \quad P_1^{01} = p_4, \\
P_1^{11} &= p_5, \quad P_1^{21} = p_6, \quad P_1^{02} = p_7, \quad P_2^{00} = p_8, \quad P_2^{01} = p_9, \\
P_2^{02} &= p_{10}.
\end{aligned} \tag{53}$$

Using the ‘‘gauge fixing’’ discussed in section Ref. 5, we can fix the phases of $f_1, f_2, f_5, f_8, f_{10}, f_{11}, f_{16}, p_0$ and A^0 to make them positive. Again, these phases are not completely independent, so the ‘‘gauge fixing’’ has to be done self-consistently.

The fixed-point conditions (eqn. (4)) form a set of non-linear equations on the variables f_i, p_i , and A^i , which can be solved exactly. After applying the ‘‘gauge fixing’’ discussed above, we find only one solution

$$\begin{aligned}
f_0 &= f_1 = \dots = f_8 = f_{16} = f_{17} = f_{18} = 1, \\
f_9 &= f_{11} = f_{14} = \frac{1}{2}, \quad f_{12} = 0, \\
f_{10} &= -f_{13} = \frac{1}{\sqrt{2}}, \quad f_{15} = -1, \\
p_1 &= p_4 = p_9 = \frac{2}{\sqrt{6}}, \quad p_5 = p_6 = 0, \\
p_0 &= p_2 = p_3 = p_7 = p_8 = p_{10} = \frac{1}{\sqrt{6}}, \\
A^0 &= A^2 = \frac{1}{\sqrt{6}}, \quad A^1 = \frac{2}{\sqrt{6}}.
\end{aligned} \tag{54}$$

We also find

$$e^{i\theta_F} = e^{i\theta_{P1}} = e^{i\theta_{P2}} = e^{i\theta_{A1}} = e^{i\theta_{A2}} = 1. \tag{55}$$

A careful comparison with Ref. 12 shows that the F -tensors obtained above perfectly match the F local rules for the $N = 2$ non-orientable string-net state in Ref. 12 (after switching the edge labels 1 and 2). Thus the above state corresponds to the standard lattice gauge theory with gauge group S_3 – the permutation group of 3 objects.

E. An $N = 2$ string-net state – the \mathbb{Z}_3 state

The above four examples all correspond to non-orientable string-net states. Here we will give an example of an orientable string-net state. We choose $N = 2$, $0^* = 0$, $1^* = 2$, $2^* = 1$, and

$$\begin{aligned} N_{000} &= N_{012} = N_{120} = N_{201} = N_{021} = N_{102} = N_{210} \\ &= N_{111} = N_{222} = 1. \end{aligned} \quad (56)$$

The above N_{ijk} satisfies eqn. (4).

This state also appeared in Ref. 12 as the other example of $N = 2$ string-net state. As in the \mathbb{Z}_2 case, the three edge labels of N form a \mathbb{Z}_3 group after we switch the definition of positive direction in the third label of N . For example, N_{012} becomes N_{011} after switching, which will then correspond to group action $0 \otimes 1 = 1$. We will call such a state the \mathbb{Z}_3 state.

Due to relation eqn. (4), different components of the tensor F_{klm}^{ijm} are not independent. There are eight independent potentially non-zero components which are denoted as f_0, \dots, f_7 :

$$\begin{aligned} F_{000}^{000} &= f_0 \\ F_{111}^{000} &= (F_{200}^{011})^* = F_{002}^{120} \\ &= (F_{020}^{202})^* = f_1 \\ F_{222}^{000} &= (F_{100}^{022})^* = (F_{010}^{101})^* \\ &= F_{001}^{210} = f_2 \\ F_{011}^{011} &= F_{022}^{022} = (F_{202}^{101})^* \\ &= (F_{101}^{202})^* = f_3 \\ F_{122}^{011} &= (F_{121}^{101})^* = F_{021}^{112} \\ &= (F_{102}^{112})^* = f_4 \\ F_{211}^{022} &= (F_{212}^{202})^* = F_{012}^{221} \\ &= (F_{201}^{221})^* = f_5 \\ F_{210}^{112} &= (F_{221}^{120})^* = (F_{112}^{210})^* \\ &= F_{120}^{221} = f_6 \\ F_{110}^{120} &= (F_{220}^{210})^* = f_7 \end{aligned} \quad (57)$$

There are nine potentially non-zero components in P_i^{kj} , which are denoted by p_0, \dots, p_8 :

$$\begin{aligned} P_0^{00} &= p_0, & P_0^{01} &= p_1, & P_0^{02} &= p_2, & P_1^{00} &= p_3, & P_1^{01} &= p_4, \\ P_1^{02} &= p_5, & P_2^{00} &= p_6, & P_2^{01} &= p_7, & P_2^{02} &= p_8. \end{aligned} \quad (58)$$

Using the ‘‘gauge fixing’’ discussed in section Ref. 5, we can fix the phases of f_1, f_2, f_6, p_0 and A^0 to make them positive.

The fixed-point conditions (eqn. (4)) form a set of nonlinear equations on the variables f_i, p_i , and A^i , which can be solved exactly. After applying the ‘‘gauge fixing’’ discussed above, we find only one solution

$$\begin{aligned} f_i &= 1, \quad i = 0, 1, \dots, 7, \\ p_i &= \frac{1}{\sqrt{3}}, \quad i = 0, 1, \dots, 8, \\ A^0 &= A^1 = A^2 = \frac{1}{\sqrt{3}}. \end{aligned} \quad (59)$$

We also find

$$e^{i\theta_F} = e^{i\theta_{P1}} = e^{i\theta_{P2}} = e^{i\theta_{A1}} = e^{i\theta_{A2}} = 1. \quad (60)$$

The fixed-point state corresponds to the \mathbb{Z}_3 string-net condensed state¹².

The process of applying the Modular transformations are exactly the same as in III A. By applying Dehn twists to all the 9 non-contractable fixed-point states on a torus, we can get the T -matrix. Note that as in III A, here all the 9 non-contractable graphs correspond to fixed-point states and are ground states of a certain local Hamiltonian. Without going into too much details, we present here the resulting 9 by 9 T -matrix:

$$T = \begin{pmatrix} 1 & 0 & 0 & 0 & 0 & 0 & 0 & 0 & 0 \\ 0 & 1 & 0 & 0 & 0 & 0 & 0 & 0 & 0 \\ 0 & 0 & 1 & 0 & 0 & 0 & 0 & 0 & 0 \\ 0 & 0 & 0 & 0 & 0 & 1 & 0 & 0 & 0 \\ 0 & 0 & 0 & 1 & 0 & 0 & 0 & 0 & 0 \\ 0 & 0 & 0 & 0 & 1 & 0 & 0 & 0 & 0 \\ 0 & 0 & 0 & 0 & 0 & 0 & 0 & 1 & 0 \\ 0 & 0 & 0 & 0 & 0 & 0 & 0 & 0 & 1 \\ 0 & 0 & 0 & 0 & 0 & 0 & 1 & 0 & 0 \end{pmatrix} \quad (61)$$

Similarly, S -matrix can be obtained by applying the 90° rotations to all the 9 fixed-point states. The resulting 9 by 9 S -matrix is then:

$$S = \begin{pmatrix} 1 & 0 & 0 & 0 & 0 & 0 & 0 & 0 & 0 \\ 0 & 0 & 0 & 0 & 0 & 0 & 1 & 0 & 0 \\ 0 & 0 & 0 & 1 & 0 & 0 & 0 & 0 & 0 \\ 0 & 1 & 0 & 0 & 0 & 0 & 0 & 0 & 0 \\ 0 & 0 & 0 & 0 & 0 & 0 & 0 & 1 & 0 \\ 0 & 0 & 0 & 0 & 1 & 0 & 0 & 0 & 0 \\ 0 & 0 & 1 & 0 & 0 & 0 & 0 & 0 & 0 \\ 0 & 0 & 0 & 0 & 0 & 0 & 0 & 0 & 1 \\ 0 & 0 & 0 & 0 & 0 & 1 & 0 & 0 & 0 \end{pmatrix}. \quad (62)$$

As before, we can choose a particular basis in which T -matrix is diagonalized and S -matrix satisfies eqn. 17 in modular tensor category theory. Without going into too much details, we present here the resulting T and

S -matrix under a change of basis:

$$T = \begin{pmatrix} 1 & 0 & 0 & 0 & 0 & 0 & 0 & 0 & 0 \\ 0 & 1 & 0 & 0 & 0 & 0 & 0 & 0 & 0 \\ 0 & 0 & 1 & 0 & 0 & 0 & 0 & 0 & 0 \\ 0 & 0 & 0 & 1 & 0 & 0 & 0 & 0 & 0 \\ 0 & 0 & 0 & 0 & \xi & 0 & 0 & 0 & 0 \\ 0 & 0 & 0 & 0 & 0 & \xi^* & 0 & 0 & 0 \\ 0 & 0 & 0 & 0 & 0 & 0 & 1 & 0 & 0 \\ 0 & 0 & 0 & 0 & 0 & 0 & 0 & \xi & 0 \\ 0 & 0 & 0 & 0 & 0 & 0 & 0 & 0 & \xi^* \end{pmatrix} \quad (63)$$

and

$$S = \frac{1}{3} \begin{pmatrix} 1 & 1 & 1 & 1 & 1 & 1 & 1 & 1 & 1 \\ 1 & 1 & 1 & \xi^* & \xi^* & \xi^* & \xi & \xi & \xi \\ 1 & 1 & 1 & \xi & \xi & \xi & \xi^* & \xi^* & \xi^* \\ 1 & \xi^* & \xi & 1 & \xi^* & \xi & 1 & \xi & \xi^* \\ 1 & \xi^* & \xi & \xi^* & \xi & 1 & \xi & (\xi)^2 & 1 \\ 1 & \xi^* & \xi & \xi & 1 & (\xi)^2 & \xi^* & 1 & \xi \\ 1 & \xi & \xi^* & 1 & \xi & \xi^* & 1 & \xi^* & \xi \\ 1 & \xi & \xi^* & \xi & (\xi)^2 & 1 & \xi^* & \xi & 1 \\ 1 & \xi & \xi^* & \xi^* & 1 & \xi & \xi & 1 & (\xi)^2 \end{pmatrix} \quad (64)$$

where $\xi = e^{i\frac{2\pi}{3}}$. As before, all information of the quasi-particles can be obtained from the above T and S matrices.

Note that the corresponding eigenvalues of T are:

$$(1, 1, 1, 1, 1, e^{i\frac{2\pi}{3}}, e^{i\frac{2\pi}{3}}, e^{-i\frac{2\pi}{3}}, e^{-i\frac{2\pi}{3}}).$$

which exactly correspond to the statistical angles of the $U(1) \times U(1)$ Chern-Simons theory^{12,17}

$$\mathcal{L} = \frac{1}{4\pi} K^{IJ} a_{I\mu} \partial_\nu a_{J\lambda} \epsilon^{\mu\nu\lambda}, \quad (65)$$

with $K = \begin{pmatrix} 0 & 3 \\ 3 & 0 \end{pmatrix}$. This is also equivalent to \mathbb{Z}_3 gauge theory.

F. $N = 3$ string-net states – the \mathbb{Z}_4 states

Now we will allow four states on each edge of the graph, namely $|0\rangle, |1\rangle, |2\rangle$ and $|3\rangle$. We will first give an example of orientable string-net state. We choose $N = 3$, $0^* = 0$, $1^* = 3$, $2^* = 2$, $3^* = 1$, and

$$\begin{aligned} N_{000} &= N_{013} = N_{130} = N_{301} = N_{022} = N_{202} = N_{220} \\ &= N_{031} = N_{103} = N_{310} = N_{112} = N_{121} = N_{211} \\ &= N_{233} = N_{323} = N_{332} = 1. \end{aligned} \quad (66)$$

The above N_{ijk} satisfies eqn. (4).

We will see that one of the solutions to be obtained corresponds to the \mathbb{Z}_4 gauge theory. Again, as in the \mathbb{Z}_3 case, the three edge labels of N form a \mathbb{Z}_4 group after switching the positive direction of the third label of N : for example, N_{121} becomes N_{123} which corresponds

to group action $1 \otimes 2 = 3$. Thus, we will call states obtained from the above fusion rules the \mathbb{Z}_4 states.

Again, due to relation eqn. (4), different components of tensor F_{klm}^{ijm} are not independent. There are now twenty independent potentially non-zero components which are denoted as f_0, \dots, f_{19} :

$$\begin{aligned} F_{000}^{000} &= f_0 \\ F_{111}^{000} &= (F_{300}^{011})^* = F_{003}^{130} \\ &= (F_{030}^{303})^* = f_1 \\ F_{222}^{000} &= (F_{200}^{022})^* = (F_{020}^{202})^* \\ &= F_{002}^{220} = f_2 \\ F_{333}^{000} &= (F_{100}^{033})^* = (F_{010}^{101})^* \\ &= F_{001}^{310} = f_3 \\ F_{011}^{011} &= F_{033}^{033} = (F_{303}^{101})^* \\ &= (F_{101}^{303})^* = f_4 \\ F_{122}^{011} &= (F_{203}^{112})^* = F_{032}^{123} \\ &= (F_{131}^{202})^* = f_5 \\ F_{233}^{011} &= (F_{121}^{101})^* = (F_{103}^{123})^* \\ &= F_{031}^{213} = f_6 \\ F_{022}^{022} &= (F_{202}^{202})^* = f_7 \\ F_{133}^{022} &= (F_{232}^{101})^* = F_{021}^{112} \\ &= (F_{102}^{213})^* = f_8 \\ F_{311}^{022} &= (F_{302}^{231})^* = (F_{303}^{303})^* \\ &= F_{023}^{332} = f_9 \end{aligned}$$

or equivalently the $U(1) \times U(1)$ Chern-Simons gauge theory:

$$\mathcal{L} = \frac{1}{4\pi} K^{IJ} a_{I\mu} \partial_\nu a_{J\lambda} \epsilon^{\mu\nu\lambda}, \quad (81)$$

with $K = \begin{pmatrix} 0 & 4 \\ 4 & 4 \end{pmatrix}$.

G. More $N = 3$ string-net states – the $\mathbb{Z}_2 \times \mathbb{Z}_2$ states

Now we will give an example of a non-orientable string-net state with four edge states. That is to set $N = 3$, $0^* = 0$, $1^* = 1$, $2^* = 2$, $3^* = 3$. We then have the following solution for N :

$$\begin{aligned} N_{000} &= N_{011} = N_{101} = N_{110} = N_{022} = N_{202} = N_{220} \\ &= N_{033} = N_{303} = N_{330} = N_{123} = N_{231} = N_{312} \\ &= N_{132} = N_{321} = N_{213} = 1. \end{aligned} \quad (82)$$

The above N_{ijk} satisfies eqn. (4).

As before, we can recognize from the above that the three edge labels of N form a $\mathbb{Z}_2 \times \mathbb{Z}_2$ group if we flip the positive direction of the third label. Since the state is non-orientable, switching the direction has no real effects. Note that any element square will give unity, which is precisely the property for group $\mathbb{Z}_2 \times \mathbb{Z}_2$.

Similarly, due to relation eqn. (4), different components of the tensor F_{klm}^{ijn} are not independent. There are now twenty-two independent potentially non-zero components which are denoted as f_0, \dots, f_{21} :

$$\begin{aligned} F_{000}^{000} &= f_0 \\ F_{111}^{000} &= (F_{100}^{011})^* = (F_{010}^{101})^* \\ &= F_{001}^{110} = f_1 \\ F_{222}^{000} &= (F_{200}^{022})^* = (F_{020}^{202})^* \\ &= F_{002}^{220} = f_2 \\ F_{333}^{000} &= (F_{300}^{033})^* = (F_{030}^{303})^* \\ &= F_{003}^{330} = f_3 \\ F_{011}^{011} &= (F_{101}^{101})^* = f_4 \end{aligned}$$

$$\begin{aligned} F_{233}^{011} &= (F_{301}^{123})^* = F_{013}^{231} \\ &= (F_{121}^{303})^* = f_5 \\ F_{322}^{011} &= (F_{201}^{132})^* = (F_{131}^{202})^* \\ &= F_{012}^{321} = f_6 \\ F_{022}^{022} &= (F_{202}^{202})^* = f_7 \\ F_{133}^{022} &= F_{023}^{132} = (F_{302}^{213})^* \\ &= (F_{212}^{303})^* = f_8 \\ F_{311}^{022} &= (F_{232}^{101})^* = (F_{102}^{231})^* \\ &= F_{021}^{312} = f_9 \\ F_{033}^{033} &= (F_{303}^{303})^* = f_{10} \\ F_{122}^{033} &= F_{032}^{123} = (F_{313}^{202})^* \\ &= (F_{203}^{312})^* = f_{11} \\ F_{211}^{033} &= (F_{323}^{101})^* = F_{031}^{213} \\ &= (F_{103}^{321})^* = f_{12} \\ F_{110}^{110} &= f_{13} \\ F_{223}^{110} &= (F_{210}^{123})^* = (F_{120}^{213})^* \\ &= F_{113}^{220} = f_{14} \\ F_{332}^{110} &= (F_{310}^{132})^* = (F_{130}^{312})^* \\ &= F_{112}^{330} = f_{15} \\ F_{123}^{123} &= (F_{213}^{213})^* = f_{16} \\ F_{132}^{132} &= (F_{312}^{312})^* = f_{17} \\ F_{220}^{220} &= f_{18} \\ F_{331}^{220} &= (F_{320}^{231})^* = (F_{230}^{321})^* \\ &= F_{221}^{330} = f_{19} \\ F_{231}^{231} &= (F_{321}^{321})^* = f_{20} \\ F_{330}^{330} &= f_{21} \end{aligned} \quad (83)$$

There are now sixteen potentially non-zero components

in P_i^{kj} , which are denoted by p_0, \dots, p_{15} :

$$\begin{aligned} P_0^{00} &= p_0, & P_0^{01} &= p_1, & P_0^{02} &= p_2, & P_0^{03} &= p_3, & P_1^{00} &= p_4, \\ P_1^{01} &= p_5, & P_1^{02} &= p_6, & P_1^{03} &= p_7, & P_2^{00} &= p_8, & P_2^{01} &= p_9, \\ P_2^{02} &= p_{10}, & P_2^{03} &= p_{11}, & P_3^{00} &= p_{12}, & P_3^{01} &= p_{13}, \\ P_3^{02} &= p_{14}, & P_3^{03} &= p_{15}. \end{aligned} \quad (84)$$

Using the ‘‘gauge fixing’’ discussed in section Ref. 5, we can fix the phases of $f_1, f_2, f_3, f_5, f_6, f_8, f_9, f_{11}, f_{12}, f_{14}, f_{16}, p_0$ and A^0 to make them positive. As before, these phases are not independent to each other, so the gauge fixing has to be done in a self-consistent way.

The fixed-point conditions (eqn. (4)) form a set of non-linear equation on the variables f_i, p_i , and A^i , which can be solved exactly. After applying the ‘‘gauge fixing’’ discussed above, we find four sets of different solutions, listing below:

$$\begin{aligned} I. \quad f_i &= 1, \quad i = 0, 1, \dots, 21, \\ p_i &= \frac{1}{2}, \quad i = 0, 1, \dots, 15, \\ A^0 &= A^1 = A^2 = A^3 = \frac{1}{2}. \end{aligned}$$

$$\begin{aligned} II. \quad f_{13} &= f_{15} = f_{17} = f_{18} = f_{19} = f_{20} = -1, \\ f_i &= 1, \quad i = \textit{otherwise}, \\ p_0 &= p_3 = p_4 = p_7 = p_8 = p_{11} = p_{12} = p_{15} = \frac{1}{2}, \\ p_1 &= p_2 = p_5 = p_6 = p_9 = p_{10} = p_{13} = p_{14} = -\frac{1}{2}, \\ A^0 &= -A^1 = -A^2 = A^3 = \frac{1}{2}. \end{aligned}$$

$$\begin{aligned} III. \quad f_{13} &= f_{15} = f_{17} = f_{21} = -1, \\ f_i &= 1, \quad i = \textit{otherwise}, \\ p_0 &= p_2 = p_4 = \dots = p_{14} = \frac{1}{2}, \\ p_1 &= p_3 = p_5 = \dots = p_{15} = -\frac{1}{2}, \\ A^0 &= -A^1 = A^2 = -A^3 = \frac{1}{2}. \end{aligned}$$

$$\begin{aligned} IV. \quad f_{18} &= f_{19} = f_{20} = f_{21} = -1, \\ f_i &= 1, \quad i = \textit{otherwise}, \\ p_0 &= p_1 = p_4 = p_5 = p_8 = p_9 = p_{12} = p_{13} = \frac{1}{2}, \\ p_2 &= p_3 = p_6 = p_7 = p_{10} = p_{11} = p_{14} = p_{15} = \frac{1}{2}, \\ A^0 &= A^1 = -A^2 = -A^3 = \frac{1}{2}. \end{aligned} \quad (85)$$

We also find

$$e^{i\theta_F} = e^{i\theta_{P_1}} = e^{i\theta_{P_2}} = e^{i\theta_{A_1}} = e^{i\theta_{A_2}} = 1. \quad (86)$$

We can further check if the results obtained above are consistent with the ones in the \mathbb{Z}_2 case (c.f. III A). A quick check can be done as follows: In III A, we have

$$f'_0 = 1 \quad \text{and} \quad f'_3 = \eta.$$

(We use f' to differentiate it from the f obtained in this section.) Since $\mathbb{Z}_2 \times \mathbb{Z}_2$ can be seen as two copies of \mathbb{Z}_2 , we expect

$$\begin{aligned} f_0 &= f_0^{a'} \times f_0^{b'} = 1, & f_{13} &= f_3^{a'} \times f_0^{b'} = \eta^a, \\ f_{18} &= f_0^{a'} \times f_3^{b'} = \eta^b, & f_{21} &= f_3^{a'} \times f_3^{b'} = \eta^a \times \eta^b. \end{aligned}$$

Thus f_{13}, f_{18}, f_{21} would either all be one, or two out of them would be -1 . This precisely corresponds to the four solutions obtained above. A more detailed check also shows consistency between the two results.

H. An $N = 3$ string-net state – the ‘‘Chiral’’ state

Finally, we present here a new state which was once thought to be a non-string-net state (but eventually turned out not to be one, fortunately or unfortunately). In this state, interestingly enough, the chiral symmetry is spontaneously broken. As before, we choose $N = 3$, $0^* = 0$, $1^* = 3$, $2^* = 2$, $3^* = 1$, and

$$\begin{aligned} N_{000} &= N_{013} = N_{130} = N_{301} = N_{123} = N_{231} = N_{312} \\ &= N_{222} = 1. \end{aligned} \quad (87)$$

The above N_{ijk} satisfies eqn. (4).

This state has several interesting features. Besides its chiral symmetry being spontaneously broken, the three edge labels of N form a structure called a ‘‘multi-fusion category’’. This mathematical structure has the following fusion rule between its four elements:

$$M_{ij} \times M_{kl} = \delta_{jk} M_{il}, \quad \text{where } i, j, k, l = 1 \text{ or } 2.$$

After making the following mapping, $M_{11} = \textit{state } 0$, $M_{12} = \textit{state } 1$, $M_{22} = \textit{state } 2$, $M_{21} = \textit{state } 3$, we can see that the fusion rule above is exactly equivalent to (87) (again, we need to flip the positive direction of the third label of N). Although the fusion rule is fairly non-trivial, we will see that at least in the no-symmetry case which we are studying in this paper, the corresponding fixed-point state is trivial.

Due to relation eqn. (4), different components of the tensor F_{klm}^{ijm} are not independent. There are now six independent potentially non-zero components which are de-

noted as f_0, \dots, f_5 :

$$\begin{aligned}
F_{000}^{000} &= f_0 \\
F_{333}^{000} &= (F_{100}^{033})^* = (F_{010}^{101})^* \\
&= F_{001}^{310} = f_1 \\
F_{233}^{033} &= (F_{323}^{101})^* = F_{011}^{211} \\
&= (F_{101}^{323})^* = f_2 \\
F_{110}^{132} &= (F_{332}^{310})^* = f_3 \\
F_{223}^{132} &= (F_{322}^{211})^* = F_{111}^{222} \\
&= (F_{232}^{323})^* = f_4 \\
F_{222}^{222} &= f_5
\end{aligned} \tag{88}$$

There are eight potentially non-zero components in P_i^{kj} , which are denoted by p_0, \dots, p_7 :

$$\begin{aligned}
P_0^{00} &= p_0, & P_0^{03} &= p_1, & P_1^{00} &= p_2, & P_1^{03} &= p_3, & P_2^{21} &= p_4, \\
P_2^{22} &= p_5, & P_3^{21} &= p_6, & P_3^{22} &= p_7.
\end{aligned} \tag{89}$$

After a gauge fixing process,⁵ we can fix the phases of f_1, f_3, f_4, p_0 and A^0 to make them positive.

The fixed-point conditions (eqn. (4)) form a set of non-linear equation on the variables f_i, p_i , and A^i , which can be solved exactly. After applying the ‘‘gauge fixing’’ discussed above, we find the solution with an undetermined parameter η :

$$\begin{aligned}
f_i &= 1, \quad i = 0, 1, \dots, 5, \\
p_0 &= p_2 = p_4 = p_6 = \eta, \\
p_1 &= p_3 = p_5 = p_7 = \sqrt{1 - \eta^2}, \\
A^0 &= \eta^2, \quad A^2 = 1 - \eta^2, \\
A^1 &= A^3 = \eta\sqrt{1 - \eta^2}.
\end{aligned} \tag{90}$$

We also find

$$e^{i\theta_F} = e^{i\theta_{P1}} = e^{i\theta_{P2}} = e^{i\theta_{A1}} = e^{i\theta_{A2}} = 1. \tag{91}$$

It can be shown that the above state corresponds to a trivial loop state with adjustable loop weights. By introducing the ‘‘double-line rule’’ and associate different weights to the ‘‘dashed-line’’ loops & ‘‘solid-line’’ loops, the state reduced to a state with independent loops. This can be seen very clearly in Fig. 2.

IV. SUMMARY

In this paper, we compute the T and S -matrices that was introduced to define topological orders in 2D.^{8,9} We argue that this new label can be used to fully describe

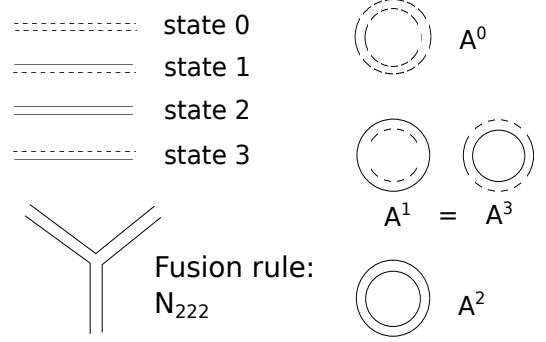


FIG. 2: The ‘‘double-line rule’’. Replace the single-line trivalence graph by double lines. If different link states are defined as shown above, then the fusion rules are automatically satisfied. (The fusion rule $N_{222} = 1$ was shown in the graph as an example.) Suppose we associate a weight η to a dashed-line loop and a weight $\sqrt{1 - \eta^2}$ to a solid-line loop respectively, then the weight of any graph can be determined. (Note that all the loops are independent, making it a trivial loop state.)

topological orders. We show explicitly how to obtain these labels from their fixed-point states by applying the ‘‘modular transformations’’. The resulting T and S -matrices are uniquely determined after a proper choice of basis and can thus be used as labels for topological orders.

The ‘‘modular transformations’’ can be defined through two transformations, *ie* the ‘‘Dehn twist’’ and ‘‘90° rotation’’. After applying both transformations in the ground-state subspace, we can get two matrices, T and S , describing ‘‘modular transformations’’. We can then change the basis to get the proper form of these two matrices.

Applying the two transformations in the ground-state subspace can be achieved by projection. We first define T and S for all non-contractable graphs on a torus, then apply unitary transformation to diagonalize the Hamiltonian. We then project T and S only onto the subspace with the smallest eigenvalue of the Hamiltonian, thus obtaining T and S for the ground states.

To get the ‘‘proper form’’ of the two labeling matrices, we first diagonalize T -matrix, and then search for unitary transformation that doesn’t change the diagonal form of T , and at the same time, make S satisfy a few requirement including the ‘‘Verlinde’’ formula (see eqn. (17)). After this unitary transformation, the form of T and S will be uniquely determined only up to permutations of basis.

The resulting T and S -matrices are unique labels for different topological orders. We believe they contain full information of the phase and can fully characterize different topological orders. Future work can be done to further generalize this method to obtain T and S matri-

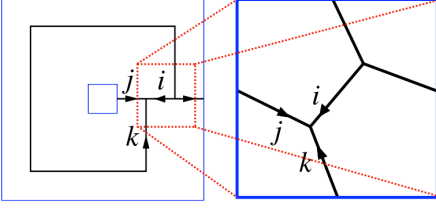


FIG. 3: (Color online) Both graphs represent non-contractable graphs on a torus. The graph on the right is a zoom-in version of the graph on the left. When constructing the Hamiltonian, we use the graph on the right to show the details of F and P -moves.

ces for general tensor-product states or other many-body states, so as to determine the topological order of an arbitrary many-body state. Even further, using this T and S -matrices description, we may eventually be able to describe phase transitions between different topological orders.

We would like to thank Z.-X. Liu, L. Kong for some very helpful discussions. This research is supported by NSF Grant No. DMR-1005541, NSFC 11074140, and NSFC 11274192. It is also supported by the John Templeton Foundation. Research at Perimeter Institute is supported by the Government of Canada through Industry Canada and by the Province of Ontario through the Ministry of Research.

Appendix A: Ideal Hamiltonian for fixed-point states on a torus

The Hamiltonian construction is similar to the one in appendix of Ref. 14. The basic idea is to construct a

Hamiltonian which is a sum of commuting projectors and is thus exactly solvable. On specific lattices for example the honeycomb lattice, it can be shown that all fixed-point wave functions $(N_{ijk}, F_{klm,\chi\delta}^{ijm,\alpha\beta}, P_i^{kj,\alpha\beta}, A^i)$ that we obtained from solving eqn. (4) are exact gapped ground states of such a local Hamiltonian.¹⁴

The Hamiltonian is of the following form:

$$\hat{H} = \sum_{\mathbf{v}} (1 - \hat{Q}_{\mathbf{v}}) + \sum_{\mathbf{p}} (1 - \hat{B}_{\mathbf{p}}) \quad (\text{A1})$$

where $\sum_{\mathbf{v}}$ sums over all vertices and $\sum_{\mathbf{p}}$ sums over all plaquettes. The Hamiltonian \hat{H} acts on the Hilbert space V_G formed by all the graph states. Operator $\hat{Q}_{\mathbf{v}}$ in \hat{H} acts on the states of the 3 links that connect to the vertex \mathbf{v} :

$$\begin{aligned} \hat{Q}_{\mathbf{v}} \left| i \begin{array}{c} \alpha \\ \downarrow \\ j \end{array} k \right\rangle &= \left| i \begin{array}{c} \alpha \\ \downarrow \\ j \end{array} k \right\rangle \quad \text{if } N_{ijk} > 0, \\ \hat{Q}_{\mathbf{v}} \left| i \begin{array}{c} \alpha \\ \downarrow \\ j \end{array} k \right\rangle &= 0 \quad \text{otherwise.} \end{aligned} \quad (\text{A2})$$

Clearly, $\hat{Q}_{\mathbf{v}}$ is a projector $\hat{Q}_{\mathbf{v}}^2 = \hat{Q}_{\mathbf{v}}$. Operator $\hat{B}_{\mathbf{p}}$ in \hat{H} acts on the states of all the links and vertices belonging to the same plaquette \mathbf{p} .

For our purpose in this paper, we only need to consider the Hamiltonian acting on the subspace of all non-contractable graphs on a torus (See Fig. 3). The $\hat{B}_{\mathbf{p}}$ operator on such a torus can be constructed from a combination of the F -moves and P -moves as follows:

$$\begin{aligned} \Phi \left(\begin{array}{c} \square \\ \text{graph} \end{array} \right) &= \sum_{t,s} (P_i^{ts})^* \Phi \left(\begin{array}{c} \square \\ \text{graph with loop} \end{array} \right) \\ &= \sum_{t,s} \sum_{i'} (P_i^{ts})^* F_{ssi'}^{i'it^*} \Phi \left(\begin{array}{c} \square \\ \text{graph with loop} \end{array} \right) \end{aligned}$$

$$\begin{aligned}
&= \sum_{t,s} \sum_{i'} \sum_{k'} (P_i^{ts})^* F_{ssi'}^{i^*it^*} F_{kj^*k'}^{i's^*i} \Phi \left(\begin{array}{c} \text{Diagram 1} \end{array} \right) \\
&= \sum_{t,s} \sum_{i'} \sum_{k'} \sum_{j'^*} (P_i^{ts})^* F_{ssi'}^{i^*it^*} F_{kj^*k'}^{i's^*i} F_{j^*ij'^*}^{k'^*s^*k^*} \Phi \left(\begin{array}{c} \text{Diagram 2} \end{array} \right) \\
&= \sum_{t,s} \sum_{i'} \sum_{k'} \sum_{j'^*} \sum_{i''} (P_i^{ts})^* F_{ssi'}^{i^*it^*} F_{kj^*k'}^{i's^*i} F_{j^*ij'^*}^{k'^*s^*k^*} F_{i'k'^*i''}^{j's^*j} \Phi \left(\begin{array}{c} \text{Diagram 3} \end{array} \right) \\
&= \sum_{t,s} \sum_{i'} \sum_{k'} \sum_{j'^*} \sum_{i''} \sum_{i'''} (P_i^{ts})^* F_{ssi'}^{i^*it^*} F_{kj^*k'}^{i's^*i} F_{j^*ij'^*}^{k'^*s^*k^*} F_{i'k'^*i''}^{j's^*j} F_{i''i'''}^{isi'} \Phi \left(\begin{array}{c} \text{Diagram 4} \end{array} \right) \\
&= \sum_{t,s} \sum_{i'} \sum_{k'} \sum_{j'^*} \sum_{i''} \sum_{i'''} \sum_{k''} (P_i^{ts})^* F_{ssi'}^{i^*it^*} F_{kj^*k'}^{i's^*i} F_{j^*ij'^*}^{k'^*s^*k^*} F_{i'k'^*i''}^{j's^*j} F_{i''i'''}^{isi'} F_{k''i'''}^{i''s^*i^*} \Phi \left(\begin{array}{c} \text{Diagram 5} \end{array} \right) \\
&= \sum_{t,s} \sum_{i'} \sum_{k'} \sum_{j'^*} \sum_{i''} \sum_{i'''} \sum_{k''} \sum_{j''} (P_i^{ts})^* F_{ssi'}^{i^*it^*} F_{kj^*k'}^{i's^*i} F_{j^*ij'^*}^{k'^*s^*k^*} F_{i'k'^*i''}^{j's^*j} F_{i''i'''}^{isi'} F_{k''i'''}^{i''s^*i^*} F_{j''i''*j''}^{k''s^*k'} \Phi \left(\begin{array}{c} \text{Diagram 6} \end{array} \right) \\
&= \sum_{t,s} \sum_{i'} \sum_{k'} \sum_{j'^*} \sum_{i''} \sum_{i'''} \sum_{k''} \sum_{j''} (P_i^{ts})^* F_{ssi'}^{i^*it^*} F_{kj^*k'}^{i's^*i} F_{j^*ij'^*}^{k'^*s^*k^*} F_{i'k'^*i''}^{j's^*j} F_{i''i'''}^{isi'} F_{k''i'''}^{i''s^*i^*} F_{j''i''*j''}^{k''s^*k'} \times \\
&\quad F_{i''i''*k''i''}^{j''s^*j''} \Phi \left(\begin{array}{c} \text{Diagram 7} \end{array} \right)
\end{aligned}$$

$$\begin{aligned}
&= \sum_{t,s} \sum_{i'} \sum_{k'} \sum_{j'^*} \sum_{i''} \sum_{i'''} \sum_{k''} \sum_{j''} (P_i^{ts})^* F_{ssi'}^{i^*it^*} F_{kj^*k'}^{i's^*i} F_{j^*ij'^*}^{k'^*s^*k^*} F_{i'k'i''}^{j's^*j} F_{i''s'i'''}^{i'si'} F_{k'^*j'k''}^{i''s^*i^*} F_{j'i''*j''}^{k''s^*k'} \times \\
&\quad F_{i''''*k''i''}^{j''s^*j''} \Phi \quad \left(\begin{array}{c} \text{Diagram 1: A square with vertices labeled } i'''' \text{ (top), } j'' \text{ (left), } i'' \text{ (right), } k'' \text{ (bottom). Lines connect } i'''' \text{ to } j'' \text{ and } i'' \text{, } j'' \text{ to } i'' \text{, } i'' \text{ to } k'' \text{, and } i'''' \text{ to } k'' \text{. A loop is formed by } i'''' \text{, } i'' \text{, and } k'' \text{.} \end{array} \right) \\
&= \sum_{t,s} \sum_{i'} \sum_{k'} \sum_{j'^*} \sum_{i''} \sum_{i'''} \sum_{k''} \sum_{j''} \sum_{t'} (P_i^{ts})^* F_{ssi'}^{i^*it^*} F_{kj^*k'}^{i's^*i} F_{j^*ij'^*}^{k'^*s^*k^*} F_{i'k'i''}^{j's^*j} F_{i''s'i'''}^{i'si'} F_{k'^*j'k''}^{i''s^*i^*} F_{j'i''*j''}^{k''s^*k'} \times \\
&\quad F_{i''''*k''i''}^{j''s^*j''} F_{si''t'}^{i''s^*i'''} P_{i''}^{t's^*} \Phi \quad \left(\begin{array}{c} \text{Diagram 2: A square with vertices labeled } i'' \text{ (top), } j'' \text{ (left), } k'' \text{ (bottom), } i'' \text{ (right). Lines connect } i'' \text{ to } j'' \text{, } j'' \text{ to } k'' \text{, and } k'' \text{ to } i'' \text{.} \end{array} \right) \quad (\text{A3})
\end{aligned}$$

thus we have the matrix \mathcal{B} given by

$$\begin{aligned}
\mathcal{B} = & \sum_{t,s} \sum_{i'} \sum_{k'} \sum_{j'^*} \sum_{i''} \sum_{i'''} \sum_{k''} \sum_{j''} \sum_{t'} (P_i^{ts})^* F_{ssi'}^{i^*it^*} F_{kj^*k'}^{i's^*i} F_{j^*ij'^*}^{k'^*s^*k^*} F_{i'k'i''}^{j's^*j} F_{i''s'i'''}^{i'si'} F_{k'^*j'k''}^{i''s^*i^*} F_{j'i''*j''}^{k''s^*k'} \times \\
& F_{i''''*k''i''}^{j''s^*j''} F_{si''t'}^{i''s^*i'''} P_{i''}^{t's^*} \quad (\text{A4})
\end{aligned}$$

which is the matrix form of operator \hat{B}_p .

Recall that all fixed-point states are exact ground states of the Hamiltonian \hat{H} defined in eqn. (A2). Thus by finding the exact ground states of \hat{H} among all the non-contractable graph states, we can find the subspace of all the fixed-point states.

In sections III B and III C, we are required to reduce the modular transformations to only within the ground-

state subspace of the above Hamiltonian. This can now be easily achieved. We can first define T and S on all the non-contractable graphs on a torus, then find the ground-state subspace by diagonalizing the Hamiltonian on these non-contractable graphic states. We can then project T and S only onto the ground-state subspace of the Hamiltonian, thus obtain the required T and S .

¹ L. D. Landau, Phys. Z. Sowjetunion **11**, 26 (1937).
² V. L. Ginzburg and L. D. Landau, Zh. Ekaper. Teoret. Fiz. **20**, 1064 (1950).
³ D. C. Tsui, H. L. Stormer, and A. C. Gossard, Phys. Rev. Lett. **48**, 1559 (1982).
⁴ R. B. Laughlin, Phys. Rev. Lett. **50**, 1395 (1983).
⁵ X. Chen, Z.-C. Gu, and X.-G. Wen, Phys. Rev. B **82**, 155138 (2010), arXiv:1004.3835.
⁶ X.-G. Wen, Phys. Rev. B **40**, 7387 (1989).
⁷ X.-G. Wen and Q. Niu, Phys. Rev. B **41**, 9377 (1990).
⁸ X.-G. Wen, Int. J. Mod. Phys. B **4**, 239 (1990).
⁹ E. Keski-Vakkuri and X.-G. Wen, Int. J. Mod. Phys. B **7**, 4227 (1993).
¹⁰ F. D. M. Haldane and E. H. Rezayi, Phys. Rev. B **31**, 2529

(1985).
¹¹ F. Wilczek and A. Zee, Phys. Rev. Lett. **52**, 2111 (1984).
¹² M. Levin and X.-G. Wen, Phys. Rev. B **71**, 045110 (2005), cond-mat/0404617.
¹³ G. Vidal, Phys. Rev. Lett. **99**, 220405 (2007).
¹⁴ Z.-C. Gu, Z. Wang, and X.-G. Wen (2010), arXiv:1010.1517.
¹⁵ E. Rowell, R. Stong, and Z. Wang (2007), arXiv:0712.1377.
¹⁶ M. Freedman, C. Nayak, K. Shtengel, K. Walker, and Z. Wang, Ann. Phys. (NY) **310**, 428 (2004), cond-mat/0307511.
¹⁷ S.-P. Kou, M. Levin, and X.-G. Wen, Phys. Rev. B **78**, 155134 (2008), arXiv:0803.2300.